

# Reinfier and Reintrainer: Verification and Interpretation-Driven Safe Deep Reinforcement Learning Frameworks

Zixuan Yang<sup>1</sup>, Jiaqi Zheng<sup>1</sup>, Guihai Chen<sup>1</sup>

<sup>1</sup>School of Computer Science, Nanjing University, Nanjing, China  
zxyang@smail.nju.edu.cn, jzheng@nju.edu.cn, gchen@nju.edu.cn

## Abstract

Ensuring verifiable and interpretable safety of deep reinforcement learning (DRL) is crucial for its deployment in real-world applications. Existing approaches like verification-in-the-loop training, however, face challenges such as difficulty in deployment, inefficient training, lack of interpretability, and suboptimal performance in property satisfaction and reward performance. In this work, we propose a novel verification-driven interpretation-in-the-loop framework *Reintrainer* to develop trustworthy DRL models, which are guaranteed to meet the expected constraint properties. Specifically, in each iteration, this framework measures the *gap* between the on-training model and predefined properties using formal verification, interprets the contribution of each input feature to the model’s output, and then generates the training strategy derived from the on-the-fly measure results, until all predefined properties are proven. Additionally, the low reusability of existing verifiers and interpreters motivates us to develop *Reinfier*, a general and fundamental tool within *Reintrainer* for DRL verification and interpretation. *Reinfier* features *breakpoints* searching and verification-driven interpretation, associated with a concise constraint-encoding language DRLP. Evaluations demonstrate that *Reintrainer* outperforms the state-of-the-art on work six public benchmarks in both performance and property guarantees. Our framework can be accessed at <https://github.com/Kurayuri/Reinfier>.

## Introduction

Recently, deep reinforcement learning (DRL) has demonstrated exceptional advancements in the development of intelligent systems across diverse domains, including game (Silver et al. 2016), networking (Luong et al. 2019), and autonomous driving (Ohn-Bar and Trivedi 2016). Nevertheless, the inherent opacity of the deep neural network (DNN) decision-making process necessitates verifiable and interpretable safety and robustness before the practical deployment (Hasanbeig, Kroening, and Abate 2020; Sriniwasan et al. 2020). Therefore, significant efforts have been invested in learning approaches integrated with formal verification to develop property-guaranteed DRL systems.

DRL properties are typically defined in terms of safety (informally, the agent never takes undesired actions), liveness (informally, the agent eventually takes desired actions), and robustness (informally, the agent takes similar actions

with perturbation in the environment) (Baier and Katoen 2008). An important approach to achieving interpretability is by addressing interpretability problems, which can evaluate the behaviors of the trained models and provide useful insight into their underlying decision-making mechanisms. Wildly concerned problems include decision boundary (identifying the boundary between different inputs that leads to different actions) (Zhang et al. 2021; Wang, Fredrikson, and Datta 2021), counterfactual explanation (identifying the counterfactual inputs that make a property unsatisfied, which highlight the system’s weaknesses) (Molnar 2020; Wachter, Mittelstadt, and Russell 2017), sensitivity and importance analysis (identifying which input feature plays a central role in the decision-making process) (De-thise, Canini, and Kandula 2019; Guidotti et al. 2018).

However, developing verifiable and interpretable DRL systems remains a technical challenge. Firstly, verification results often serve only as adversarial counterexamples (Madry et al. 2017; Jin et al. 2022; Clarke et al. 2003; Xie et al. 2019) or just indicate whether the training process should be prolonged, leading to inefficient interaction and lengthy training time. For instance, the verification-in-the-loop approaches, where the model is alternately trained and verified against properties in each iteration until all predefined properties are proven (Jin et al. 2022; Gross et al. 2022; Amir et al. 2023; Zhang et al. 2023), rely on a single counterexample derived from time-consuming verification for property learning, making the process inefficient. Secondly, our evaluation results reveal that existing approaches fall short in terms of both property satisfaction and reward performance. Lastly, interpretability, a widely-concerned factor in developing trustworthy DRL systems, is overlooked.

In this paper, we propose a novel verification-driven interpretation-in-the-loop framework *Reintrainer* (Reinforcement Trainer) that can develop reliable DRL systems with verifiable and interpretable guarantees. Specifically, we design the *Magnitude and Gap of Property Metric* algorithm integrated with reward shaping (Ng, Harada, and Russell 1999) strategies during training. This algorithm leverages the *gap* (the difference between the current training model and the predefined properties), and the *density* (each input feature’s contribution metric to the model’s output based on interpretability), to measure the magnitudes of violations, i.e. the distances between the boundary of the property-

constrained spaces and the states where violations occur. We measure the *gap* through introducing *breakpoint* searching, which involves finding the properties whose adjacent parameters’ differences lead to the reverse verification results, i.e., from Proven to Falsified or vice versa. The identified *breakpoints* corresponds to the strictest states where the model can maintain predefined safety, liveness, or robustness, providing accurate and persuasive metrics in evaluating how safe and robust the on-training DRL model is.

Meanwhile, the existing verifiers and interpreters (Kazak et al. 2019; Eliyahu et al. 2021; Amir, Schapira, and Katz 2021; Ivanov et al. 2021; Huang et al. 2023) lack reusability for DRL system designers and are limited in the types of properties and interpretability questions they can address, which hinders their effectiveness and applicability. To address this, we design and implement a verifier and interpreter named *Reinfier* (Reinforcement Verifier) that serves as the backend of *Reintrainer* or can be used as an independent tool. *Reinfier* can answer various interpretability questions by searching for *breakpoints* effectively. Although we can use programming languages like Python to encode DRL properties, interpretability questions, and training constraints separately, the additional learning cost and workload from hardcoding and repetitive coding are significant. Therefore, we present DRLP, a language that allows encoding them in a single, independent, configurable script with a unified format and clean, straightforward syntax.

We implement *Reintrainer* in Python, seamlessly integrable with popular vanilla DRL algorithms such as DDPG (Lillicrap et al. 2015). Different from the state-of-the-art (SOTA) verification-in-the-loop approach (Jin et al. 2022), resizing the DNN with a specialized data structure to map the environment state to the DNN input, *Reintrainer* is completely decoupled from the DRL model structures and thus deployment-friendly. Furthermore, the training process and trained model of *Reintrainer* are inherently interpretable and are adapted to endorsed DRL training frameworks, such as Stable-Baselines (Raffin et al. 2021), making the transformation of vanilla training into property-constrained training a non-burdensome task.

We evaluate *Reintrainer* on six classic control tasks in public benchmarks. For each task, we train DRL systems under identical settings in *Reintrainer*, the SOTA approach (Jin et al. 2022), and the corresponding vanilla DRL algorithm. Experimental results show that the systems trained in *Reintrainer* present superior reward performance and satisfaction guarantee of properties. We also assess *Reinfier* on a widely used case study, yielding valuable insights.

Collectively, our contributions are enumerated as follows:

- *Reintrainer*, a novel verification-driven interpretation-in-the-loop framework with the *Magnitude and Gap of Property Metric* algorithm to develop reliable DRL systems.
- *Reinfier*, a verifier and interpreter featuring *breakpoints* searching and a cohesive methodology to address interpretability problems using identified *breakpoints*.
- DRLP, a concise and unified language for DRL properties, interpretability questions, and training constraints, designed for simplicity and readability.

- Evaluation of our implementations, demonstrating that *Reintrainer* outperforms the SOTA on public benchmarks, while *Reinfier* effectively verifies key properties and provides valuable interpretability insights.

## Preliminaries

**Markov Decision Process (MDP).** An MDP is defined as  $M = \langle S, A, T, \gamma, r \rangle$ .  $S$  is the state space;  $A$  is the action space;  $T = \{P(\cdot|s, a) : s \in S, a \in A\}$  is the transition dynamics, and  $P(s'|s, a)$  is the probability of transition from state  $s$  to state  $s'$  when the action  $a$  is taken;  $r : S \times A \rightarrow \mathbb{R}$  is the reward function;  $\gamma \in [0, 1)$  is the discount factor.  $I \subseteq S$  is the initial state space. A policy  $\pi : S \rightarrow A$  defines that the decision rule the agent follows. The goal in DRL is to learn an optimal policy maximizing the expected discounted sum of rewards, i.e.,  $\arg \max_{\pi} \mathbb{E}_{\tau \sim \pi} [\sum_{t=0}^{\infty} \gamma^t r(s_t, a_t)]$ , where  $t$  denotes the timestep,  $\tau$  denotes a trajectory  $(s_0, a_0, s_1, \dots)$ , and  $\tau \sim \pi$  indicates the distribution over trajectories depends on the policy  $\pi$ .

**Formal Verification of DRL Systems.** Given a DRL system whose policy is modeled by a DNN  $N$ , a property  $\phi$  defines a set of constraints over the input  $x$  and the output  $N(x)$  (or denoted by  $y$ ). Verifying such a system aims to prove or falsify :  $\forall x \in \mathbb{R}^n, P(x) \Rightarrow Q(N(x))$  (for all  $x$ , if pre-condition  $P(x)$  holds, post-condition  $Q(N(x))$  is also satisfied) (Landers and Doryab 2023). For simplicity, the agent’s policy  $\pi$  is consistent with its DNN  $N$ , and the state  $s$  input to the policy is consistent with the input  $x$  of the DNN. In this paper,  $k$  denotes the verification depth (the maximum timestep limitation considered in verification), and  $n$  denotes the number of the state features.

In the properties of formal verification (e.g.,  $\phi \equiv s \in [(1, 2), (3, 4)] \Rightarrow a \in [0, +\infty)$ ), the property-constrained spaces consist of the constraint intervals (e.g.,  $\phi[s] = [(1, 2), (3, 4)]$ , where  $\phi[s]$  denotes the constraint interval of the state  $s$  in property  $\phi$ , indicating the 0th feature of the state  $s^0 \in [1, 3]$  and the 1st feature  $s^1 \in [2, 4]$ , rather than concrete system states and actions (e.g.,  $s = \langle 1, 2 \rangle$ ). Further,  $\underline{\phi}[s]$  donates the lower bounds of the constraint interval of the state, while  $\overline{\phi}[s]$  donates the upper bounds. The properties of verification can be formulated using satisfiability modulo theories (SMT) expressions, and the sets and functions defined in  $M$  can be treated as predicates; for example, when  $s \in S$ , predicate  $S(s)$  is True, or when  $T(s'|s, a) > 0$ , predicate  $T(s, s')$  is True.

## Framework Overview

Fig. 1 shows the overview of *Reintrainer* consisting of three sequential stages in every iteration:

(i) **Training stage:** This stage consists of several training epochs. After several epochs, the model is updated and we move to the verification stage. Specifically, in every epoch, the model is rolled out in the environment, and we obtain set of trajectories  $\{\tau_i\}$  stored in the buffer. Subsequently, within the experiences of each trajectory, we measure the magnitude of violation or satisfaction of the predefined properties in DRLP and trace back the sequence leading to viola-

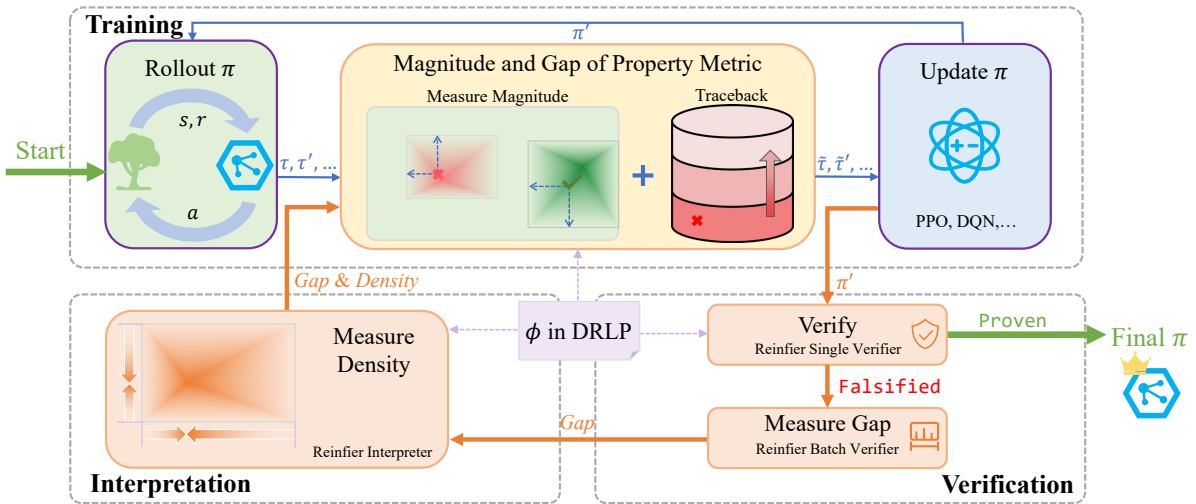


Figure 1: Reintrainer architecture.

tion or satisfaction. Accordingly, we modify the corresponding reward of each experience following our generated reward shaping strategy. Finally, we update the model based on DRL algorithms such as PPO (Schulman et al. 2017), and proceed to the next epoch. In addition to reward shaping, our metric result might also be considered as the cost in Constrained MDP to integrate with advanced optimization algorithms in the future.

(ii) **Verification stage:** We verify the predefined DRLP properties through *Reinifier* on the model. If all properties are proven and the model is converged, we stop the iterations and return the model. Otherwise, we measure the *gap* between the model and predefined properties.

(iii) **Interpretation stage:** We interpret the model through *Reinifier* to measure the *density* of state features within the constraint space defined by given properties in DRLP. Later, we generate a reward shaping strategy based on the *density* and the *gap* for the training, and then we return to the training stage to resume training the model.

Our measure and modification are entirely decoupled from the vanilla algorithms. The integration of training, verification, and interpretation seamlessly constitutes a verification-driven interpretation-in-the-loop DRL approach. After several iterations, *Reintrainer* can develop well-performing, property-compliant, verification-guaranteed, and interpretable models.

### Design of Verifier and Interpreter

We design and implement *Reinifier*, which achieves functions far beyond *Reintrainer*’s requirements and also addresses the challenges of reusability and completeness in terms of the type of properties as well as interpretability questions. Therefore, it can also be used as an independent and user-friendly tool for DRL verification and interpretation. We introduce novel concepts in the main text, while the detailed functional design is provided in Appendix C.

Fig. 2 shows the working procedure of *Reinifier*. To avoid reinventing the wheel, we opt to use existing DNN verifiers

DNNV (Shriver, Elbaum, and Dwyer 2022), Marabou (Katz et al. 2019) and Verisig (Ivanov et al. 2021) as the DNN verification backend. A parser for given properties in DRLP and an adapter for given DNN models designed and implemented by us function as intermediaries, bridging *Reinifier* with the DNN verifiers. We implement the single verifier by realizing model-checking algorithms or using reachability analysis, obtaining conventional Boolean DRL verification results (whether properties hold or not) derived from previous DRL verification works (Eliyahu et al. 2021; Ivanov et al. 2021). Building upon this foundation, we introduce the novel *batch* verifier, featuring *breakpoints* searching on the DRLP templates. The numeric DRL verification results from our *batch* verifier provide a more accurate measure of the DRL model’s safety and robustness. Additionally, our interpreter for answering interpretability questions features a cohesive methodology and corresponding solutions based on the identified *breakpoints*.

### Descriptive Language: DRLP

The detailed syntax of DRLP is defined in Appendix B. A DRLP verification script can be structurally divided into three segments. The first segment initializes a series of pre-assigned variables used for the verification. The second segment, starting with a delimiter @Pre, is a set of the pre-conditions  $P$  (the prerequisite of properties). The third segment, starting with a delimiter @Exp, is a set of the post-conditions  $Q$  (the expected results). In the script,  $x$  denotes the input of DNN,  $y$  denotes the output of DNN, and  $k$  denotes the verification depth; variables prefixed with “\_” are categorized as *iterable variables*. Fig. 3 shows four verification scripts encoded with the properties and a DRL system with two state features and one continuous action.

**Safety and Liveness Property.** A verification script on the safety property is shown in Fig. 3(a). We first detail pre-conditions (Line 3-7). Each state feature  $x$  belongs to the interval  $[-1, 1]$  (Line 3). Considering two cases that  $a$  equals 0 or 1 (Line 1), the value of each initial state feature is re-

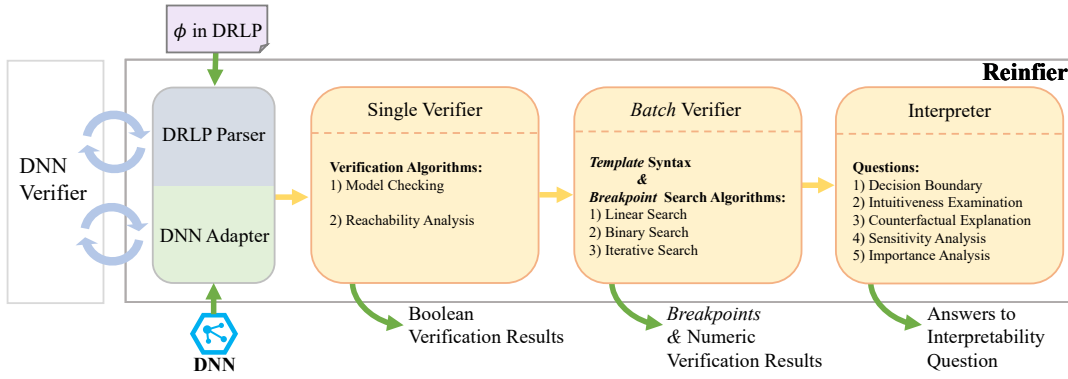


Figure 2: Working procedure of Reinfier.

<pre> 1  _a = [0,1] 2  @Pre 3  [[-1]*2]*k &lt;= x &lt;= [[1]*2]*k 4  [a]*2 == x[0] 5  for i in range(0,k-1): 6    Implies(y[i] &gt; [0], x[i]+0.5 &gt;= x[i+1] &gt;= x[i]) 7    Implies(y[i] &lt;= [0], x[i]-0.5 &lt;= x[i+1] &lt;= x[i]) 8 9 10 @Exp 11 y &gt;= [[-2]]*k 12 </pre>	<pre> 1  _a = [0,1] 2  @Pre 3  [[-1]*2]*k &lt;= x &lt;= [[1]*2]*k 4  [a]*2 == x[0] 5  for i in range(0,k-1): 6    Implies(y[i] &gt; [0], x[i]+0.5 &gt;= x[i+1] &gt;= x[i]) 7    Implies(y[i] &lt;= [0], x[i]-0.5 &lt;= x[i+1] &lt;= x[i]) 8    for i in range(0,k-1): 9      x[i] != x[k-1] 10 @Exp 11 for i in orange(0, k): 12   y[i] &gt;= [[-2]]*k </pre>	<pre> 1  _x_eps = [0.01, 0.1] 2  y_eps = 0.2 3  y_original = 0 4  @Pre 5  [1, 0] - x_eps &lt;= x[0] &lt;= [1, 0] + x_eps 6 7 8 9 10 @Exp 11 y_original - y_eps &lt;= y[0] &lt;= y_original + y_eps </pre>	<pre> 1  _x_eps = [10, 20] 2  y_eps = 1 3  y_original = 0 4  @Pre 5  [1- x_eps, 0] &lt;= x[0] &lt;= [1 + x_eps, 0] 6 7 8 9 10 @Exp 11 y_original - y_eps &lt;= y[0] &lt;= y_original + y_eps 12 </pre>
(a) Safety	(b) Liveness	(c) Local robustness	(d) Extreme value robustness

Figure 3: Illustration of four verification scripts characterizing the properties of (a) safety, (b) liveness, (c) local robustness and (d) extreme value robustness.

spectively 0 or 1 (Line 4). Note that each value of the next state increases by at most 0.5 if the action is greater than 0 (Line 5,6), and decreases by at most 0.5 otherwise. The post-condition is that the action should always be not less than  $-2$  (Line 11). Different from the safety one, the liveness property (Fig. 3(b)) enforces the additional pre-conditions that no state cycle exists (Line 8,9) and the post-condition is that the action should be eventually not less than  $-2$  (Line 11,12).

**Robustness Property.** A verification script on the local robustness property is shown in Fig. 3(c). The pre-condition is that considering two degrees of perturbations  $x\_eps$  (equals 0.01 or 0.1) respectively (Line 1), each input feature is perturbed accordingly (Line 5). The post-condition (Line 11) is that the output’s deviation to its original output  $y\_original$  (equals 0) should not exceed  $y\_eps$  (equals 0.2). Another script on extreme value robustness is shown in Fig. 3(d). The pre-condition is that considering two degrees of outliers  $x\_eps$  (equals 10 or 20) respectively (Line 1), only the first input feature is the outlier while the second is not (Line 5). The post-condition (Line 11) is that the output’s deviation to its original output  $y\_original$  (equals 0) should not exceed  $y\_eps$  (equals 1).

### Batch Verifier

A DRLP template is a type of DRLP script characterized by the inclusion of inconcrete parameters (i.e., variables rather than specific values) and is typically derived from a

qualitative property. The scripts depicted in Fig. 3 excluded by the first segment can be viewed as templates. By iterable variables or feeding a sequence of parameter values, each template can be concretized (replacing variables with specific values) into concrete scripts for multiple cases.

We introduce the *breakpoints* search algorithm, as outlined in Algorithm 1, which leverages single verification along with a combination of binary and linear search to identify *breakpoints* on DRLP templates. The algorithm’s general form is in Appendix C.4. The identified *breakpoints* correspond to the strictest states where the model can maintain predefined properties. For example, the target model should satisfy the safety property  $\phi \equiv x > 0 \Rightarrow N(x) > 0$ . However, identified *breakpoints* reveals that initially, the strictest property that the model satisfies is  $\phi \equiv x > 0 \Rightarrow N(x) > -5$ , and then advances to  $\phi \equiv x > 0 \Rightarrow N(x) > -2$ . These numeric verification results extracted from the parameters in the properties, specifically  $-5$  and  $-2$ , demonstrate that the model is progressively becoming safer, indicating the efficacy of the preceding training strategy.

### Interpreter

Our proposition introduces a cohesive methodology to these problems, fundamentally reliant on the identified *breakpoints*. This methodology has the potential to address a broader spectrum of interpretability concerns. Specifically, we propose novel *breakpoints*-based solutions for five in-

---

**Algorithm 1: FindBreakpoints**


---

**Input:** DRLP template  $p$ , DNN  $N$ , variable list  $\{var\}$ 
**Output:** Breakpoint list  $\{bp\}$ 

```

1:  $var \leftarrow$  pop the top variable from  $\{var\}$ 
2:  $lb \leftarrow$  the lower bound of  $var$ ,  $ub \leftarrow$  the upper bound of  $var$ 
3:  $prec \leftarrow$  the search precision of  $var$ 
4:
5: if  $\{var\}$  is empty then
6:    $lb\_r, violation \leftarrow$  verify(concretize( $p, var, lb$ ),  $N$ )
7:    $ub\_r, violation \leftarrow$  verify(concretize( $p, var, ub$ ),  $N$ )
8:   while  $ub - lb \geq prec$  and  $lb\_r \neq ub\_r$  do
9:      $curr \leftarrow \frac{lb+ub}{2}$ 
10:     $script \leftarrow$  concretize( $p, var, curr$ )
11:     $curr\_r, violation \leftarrow$  verify( $script, N$ )
12:    if  $curr\_r = \text{Falsified}$  then
13:       $curr \leftarrow$  the value of  $var$  in  $violation$ 
14:    end if
15:    if  $curr\_r = lb\_r$  then:  $lb \leftarrow curr$ 
16:    else if  $curr\_r = ub\_r$  then:  $ub \leftarrow curr$ 
17:  end while
18:  Add  $script$ 's corresponding property to  $\{bp\}$ 
19: else
20:   while  $ub - lb \geq prec$  do
21:      $script \leftarrow$  concretize( $p, var, lb$ )
22:     FindBreakpoints( $script, N, \{var\}$ )
23:      $lb \leftarrow lb + prec$ 
24:   end while
25: end if

```

---

interpretability problems, including decision boundary, intuitiveness examination, counterfactual explanation, sensitivity analysis, and importance analysis. Except for the sensitivity analysis, which is related to the metric of *density*, the other four solutions are provided in Appendix C.5.

**Sensitivity Analysis** Given the original input  $x_0$  and the perturbation  $\varepsilon$ , the sensitivity analysis question (Dethise, Canini, and Kandula 2019) aims to evaluate the distances between  $N(x_0)$  and  $N(\hat{x}_0)$ , where  $x_0$  denotes the input whose features under discussion are subjected to the perturbation  $\varepsilon$ . Sensitivity analysis conducted on all input features reveals which specific feature, with a higher sensitivity result, has the potential to induce greater fluctuations in the output.

**Our solution:** Find *breakpoints* by stepping through possible  $y_0$  on the property formulated as:

$$\forall x_0, \bigwedge_{j \in D} (\hat{x}_0^j - \varepsilon \leq x_0^j \leq \hat{x}_0^j + \varepsilon) \wedge \bigwedge_{j \in R} (\hat{x}_0^j = x_0^j) \Rightarrow N(x_0) \approx y_0 \quad (1)$$

where  $D$  denotes the set of indices of the discussed features within the input, while  $R$  denotes the set of indices of other features. Finally, the answer is the minimum distance between  $y_0$  and  $N(\hat{x}_0)$ , i.e., sensitivity, formulated as:  $\min_{bp \in \{bp\}} d(y_0, N(\hat{x}_0))$ .

### Magnitude and Gap of Property Metric Algorithm

The hypothesis we advocate posits that penalties (reward reductions applied to discourage undesired actions) are di-

rectly proportional to the magnitude of violations. Furthermore, this proportionality extends to the deviation from current states to those states where the property holds. This deviation can be equivalently described as the distance between the boundary of the property-constrained spaces and the states where violations occur. The theoretical proof that our hypothesis and algorithm for property learning do not affect the optimality of the policy is provided in Appendix A.2. Additional details are provided in Appendix D.

### Distance of States

**Distance density.** The concept of sensitivity analysis in Sensitivity Analysis inspires us that the fluctuations in the output could be different for the same input feature at different values, thus we introduce the *distance density* considering that perturbations only need evaluating in one direction at the boundary: given the DNN  $N$  and the property  $\phi$ , when the input feature  $s_i^j$  is subject to perturbation  $\varepsilon$ , the *density* of the lower bound  $\underline{\rho}(\phi, s_i^j)$  can be formulated as:

$$\underline{\rho}(\phi, s_i^j) = \max_s d(N(\phi[s_i]), N(s)) \quad (2)$$

where  $s \in [\langle \phi[s_i^0], \dots, \phi[s_i^j], \dots, \phi[s_i^{n-1}] \rangle, \langle \phi[s_i^0], \dots, \phi[s_i^j] + \varepsilon, \dots, \phi[s_i^{n-1}] \rangle]$ . The upper bound *density* function  $\bar{\rho}$  can be defined similarly.

**Exact middle point.** The exact middle point, denoted as  $\dot{\phi}[s_i^j]$ , represents the position with the maximum distance to the boundary, and also the point where the *density* of the lower and upper boundaries switches. Consequently, the exact middle point  $\dot{\phi}[s_i^j]$  is the midpoint of the *density*-weighted upper and lower bounds, formulated as:

$$\dot{\phi}[s_i^j] = \frac{\underline{\rho}(\phi, s_i^j) \cdot \phi[s_i^j] + \bar{\rho}(\phi, s_i^j) \cdot \bar{\phi}[s_i^j]}{\underline{\rho}(\phi, s_i^j) + \bar{\rho}(\phi, s_i^j)} \quad (3)$$

**Distance of States in 1-Dimension** Given the state feature  $s_i^j$  whose current observation is  $\mathbf{v}$ , its normalized distance  $dist$  to its property-constrained space  $\phi[s_i^j]$  in 1-dimension is formulated as:

$$dist(\phi[s_i^j], \mathbf{v}) = \begin{cases} \left( \frac{\mathbf{v} - \underline{\phi}[s_i^j]}{\underline{\phi}[s_i^j] - \dot{\phi}[s_i^j]} \right)^{p_1} & \text{if } \mathbf{v} \in [\underline{\phi}[s_i^j], \dot{\phi}[s_i^j]] \\ \left( \frac{\bar{\phi}[s_i^j] - \mathbf{v}}{\bar{\phi}[s_i^j] - \dot{\phi}[s_i^j]} \right)^{p_1} & \text{if } \mathbf{v} \in (\dot{\phi}[s_i^j], \bar{\phi}[s_i^j]] \\ 0 & \text{else} \end{cases} \quad (4)$$

where  $p_1$  represents the penalty intensity coefficient, and we typically set  $p_1$  to 1.

**Distance of States in  $n$ -Dimension** Considering the differences in input feature to affect the outputs, we employ a *density*-weighted  $\ell^{p_2}$ -norm. Given the state  $s$  whose current observation is  $\mathbf{s}$ , its distance  $Dist$  to the property-constrained space  $\phi$  is formulated as:

$$Dist(\phi, \mathbf{s}) = \frac{\sqrt[p_2]{\sum [\underline{\rho}(\phi, s_i^j) \cdot (dist(\phi[s_i^j], \mathbf{s}_i^j))^{p_2}]}}{\sum \rho(\phi, s_i^j)} \quad (5)$$

where  $p_2$  is typically set to 2;  $\rho(\phi, s_i^j)$  equals  $\underline{\rho}(\phi, s_i^j)$  when  $s_i^j < \hat{\phi}[s_i^j]$ , otherwise, it equals  $\bar{\rho}(\phi, s_i^j)$ .

### Metric of Violation’s or Satisfaction’s Magnitude.

For the vast majority of cases, setting the distance of actions to a fixed value is sufficient. However, similarly, it can also be calculated as the distance of states. Given the observed environmental state  $\mathbf{s}$  and the action taken  $\mathbf{a}$ , we measure the magnitude of violation(−) or satisfaction(+) when the property  $\phi$  is violated or satisfied, which is formulated as:

$$Diff(\phi, \mathbf{s}, \mathbf{a}) = \pm Dist(\phi, \mathbf{s}) \cdot Dist(\phi[\mathbf{a}], \mathbf{a}) \quad (6)$$

### Metric of the Gap

We introduce the concept of *gap* to quantitatively measure the divergence between the anticipated parameter specified in the predefined property and the identified *breakpoints* from the on-training model. The high computational complexity of finding *breakpoints* confines the *gap* measurement to just one parameter  $z$  from the state features or the action.

**Definition 1.** Property  $\hat{\phi}$  is a relaxation of property  $\phi$ , if and only if  $\phi \Rightarrow \hat{\phi}$ .

**Theorem 1.** Property  $\hat{\phi} \equiv \hat{P} \Rightarrow \hat{Q}$  is a relaxation of property  $\phi \equiv P \Rightarrow Q$ , if  $\hat{P} \subseteq P, \hat{Q} \supseteq Q$ .

In this context, we find *breakpoints* by stepping through  $z$  within the  $\phi$ ’s relaxation domain  $\hat{\Phi}_{\phi \equiv P \Rightarrow Q} = \{\hat{P} \Rightarrow \hat{Q} : \forall \hat{P}, \hat{Q}, \hat{P} \subseteq P, \hat{Q} \supseteq Q\}$  on DNN  $N$ . Subsequently,  $\{bp\}$  denotes the identified *breakpoints*, and the *gap* function is formulated as:

$$g(\phi, N) = \min_{\hat{\phi} \in \{bp\}} |\phi[z] - \hat{\phi}[z]| \quad (7)$$

The *gap* metric can serve as an indicator for property learning and can also be combined with a learning rate schedule function  $Lr$  as:  $F_t = Lr(g(\phi, N)) \times Diff(\phi, \mathbf{s}, \mathbf{a})$ .

### Traceback

For properties that span multiple steps, including multi-step safety and liveness, violation occurring at a particular step implies increasing unsafety in the preceding trajectory. Therefore, it is imperative to trace back to adjust the reward trajectories in the buffer before policy optimization. For action avoidance property, we calculate the traced intermediate reward  $\tilde{F}_t$  backward from the last trajectory in the buffer with a discount factor  $\mu \in [0, 1)$  as:  $\tilde{F}_t = F_t - \lambda^{-1}F_{t-1} + \mu\tilde{F}_{t+1}$ ; for destination reach property,  $\tilde{F}_t = \lambda F_{t+1} - F_t + \mu\tilde{F}_{t+1}$ . The final shaped reward given to the agent  $\tilde{r}_t$  is formulated as:  $\tilde{r}_t = r_t + \tilde{F}_t$ .

## Evaluation

The evaluation of *Reinfier*, the supplementary and the ablation studies of *Reintrainer* are provided in Appendix E.

**Benchmarks and Experimental Settings.** We evaluate *Reintrainer* on the same six public benchmarks used in Trainify (Jin et al. 2022). Mountain Car (MC) (Moore 1990) task consists of a car placed at the bottom of a valley, and its

goal is to accelerate the car to reach the top of the right hill. Cartpole (CP) (Barto, Sutton, and Anderson 1983) task consists of a pole attached by an unactuated joint to a cart, which moves along a frictionless track, and its goal is to balance the pole. Pendulum (PD) (Brockman et al. 2016) task consists of a pendulum attached at one end to a fixed point while the other end is free and starts in a random position, and its goal is to apply torque on the free end to swing it into an upright position. B1 and B2 (Ivanov et al. 2021; Gallestey and Hokayem 2019) are two classic nonlinear systems, where agents in both systems aim to arrive at the destination region from the preset initial state space. Tora (Jankovic, Fontaine, and Kokotović 1996) task consists of a cart attached to a wall with a spring, and inside which there is an arm free to rotate about an axis; its goal is to stabilize the system at the stable state where all the system variables are equal to 0.

All experiments are conducted on a workstation with two 8-core CPUs at 2.80GHz and 256 GB RAM. We adopt the same training configurations for each task respectively.

For each task, we predefine certain properties related to their safety or liveness. All these properties, along with their types and meanings, are presented in Table 1, and their definitions are provided in Appendix E.2.4. *Reintrainer* can automatically translate DRLP scripts, encoded from predefined properties, into violation measure strategies at runtime.

We employ the DQN algorithm (Mnih et al. 2013) for tasks MC and CP with discrete actions, while we employ the DDPG algorithm (Lillicrap et al. 2015) for the other four tasks with continuous actions. For tasks MC, CP, and PD, all training hyperparameters for vanilla algorithms are finely tuned to achieve their optimal performance, and *Reintrainer* directly employs these same hyperparameters. We train two specific types of Trainify: Trainify#1 employs the hyperparameters from its original work, and Trainify#2 employs the same hyperparameters as the vanilla algorithms. For tasks B1, B2 and Tora, we employ the total same hyperparameters from the work of Trainify for Reintrainer, vanilla algorithms and Trainify#1.

**Final Model Comparison.** We evaluate the final models in their environments for 100 episodes, and calculate the average and standard deviation of the cumulative rewards, as shown in Table 2. The results demonstrate that our approach significantly outperforms both types of Trainify and even fine-tuned vanilla algorithms in all cases. We also formally verify the predefined properties on the final models. The results in Table 2 show that the vanilla algorithms do not guarantee these properties to be satisfied, while in some cases the property is naturally satisfied. The final models trained by Trainify fail to satisfy certain properties, a shortfall we attribute to the inherent limitations of its method, which primarily focuses on subdividing the abstract state space based on counterexamples but lacks mechanisms to prevent the agent from taking unexpected actions, a critical aspect for ensuring safety. In contrast, Trainify performs well in terms of reachability properties, such as  $\phi_4$  and  $\phi_5$ , enabling the agent to reach specific states. The evaluation results of the final models reveal that our approach guarantees property satisfaction without incurring performance penalties com-

Task	Type	ID	Meaning
MC	Safety	$\phi_1$	When the car is moving right at high speed at the bottom of the valley, it should not accelerate to the left.
CP	Safety	$\phi_2$	When the car is moving right in the left edge area and the pole tilts right at a large angle, it should be pushed to the right.
PD	Safety	$\phi_3$	When the pendulum approaches the upright position of the target, large torque should not be applied.
B1	Liveness	$\phi_4$	The agent always reaches the target eventually.
B2	Liveness	$\phi_5$	The agent always reaches the target eventually.
Tora	Safety	$\phi_6$	The agent always stays in the safe region.

Table 1: Predefined properties of benchmarks.

Task	MC		CP		PD		B1		B2		Tora			
	$2 \times 256$		$2 \times 256$		[300, 400]		$2 \times 20$		$2 \times 20$		$3 \times 100$		$3 \times 200$	
Network	$\bar{R} \pm \sigma$	V.R.	$\bar{R} \pm \sigma$	V.R.	$\bar{R} \pm \sigma$	V.R.	$\bar{R} \pm \sigma$	V.R.	$\bar{R} \pm \sigma$	V.R.	$\bar{R} \pm \sigma$	V.R.	$\bar{R} \pm \sigma$	V.R.
Reinfier (Ours)	-101.92±7.36	✓	500.00±0.00	✓	-132.88±85.83	✓	-119.14±0.99	✓	-20.77±0.95	✓	-50.00±0.00	✓	-50.00±0.00	✓
Trainify#1	-103.81±13.21	×	500.00±0.00	×	-328.86±189.71	✓	-122.00±0.00	✓	-23.72±0.69	✓	-50.00±0.00	×	-50.00±0.00	×
Trainify#2	-116.21±4.00	×	500.00±0.00	×	-354.52±189.94	✓	-	-	-	-	-	-	-	-
Vanilla	-103.82 <sub>pm</sub> 9.37	×	500.00±0.00	×	-142.90±86.21	✓	-122.00±0.00	✓	-20.85±0.88	✓	-50.00±0.00	×	-50.00±0.00	×

Table 2: Comparison of the final models.  $\bar{R} \pm \sigma$  stands for the average episode reward and its standard deviation of the final models’ evaluation results. **V.R.** stands for verification result, where ✓ indicates that the predefined property is proven, while × indicates falsification.

pared to the vanilla algorithms. Additionally, our approach outshines Trainify by demonstrating superior performance, guaranteeing satisfaction across a wider variety of property types, and high efficiency in terms of training timesteps.

## Related Work

Numerous safe DRL methods have been proposed to ensure DRL safety. The most popular methods are constrained optimization-based safe DRL, which focus on optimizing the agent’s behavior while adhering to safety constraints through Lagrangian relaxation (Ray, Achiam, and Amodei 2019; Jiaming Ji 2023) and constrained policy optimization (Yang et al. 2022, 2020; Achiam et al. 2017). However, they only minimize the cost of unsafe actions during training and cannot guarantee absolute safety in deployment.

Formal verification-based methods can rigorously ensure learning safety compared to the aforementioned methods. Among these, verification-in-the-loop training, rather than train-then-verify, can more efficiently train models. The pioneering work (Nilsson et al. 2015) proposes a correct-by-construction approach for developing Adaptive Cruise Control by defining safety properties and computing the safe domain. Trainify (Jin et al. 2022) develops DRL models driven by counterexamples, refining abstract state space, which limits model structure and is highly inefficient. COOL-MC (Gross et al. 2022) combines a verifier and training environments without any safe learning method. The work (Amir et al. 2023) leverages verifiers to select the best available policy and continues training on the chosen policy.

Moreover, interpretability is another method to indirectly enhance model safety. DRL interpretability focuses on explaining the decision-making rules of models (Meng et al. 2020; Zhang et al. 2021; Wachter, Mittelstadt, and Russell 2017; Lee and Landgrebe 1997) and analyzing model characteristics (Dethise, Canini, and Kandula 2019; Molnar 2020; Guidotti et al. 2018). UINT (Huang et al. 2023) first proposes that several interpretability questions can be for-

mulated in SMT problem format, similar to verification. Our interpreter expands the types of questions and features an integration of more types of properties and problems.

The methods mentioned above do not explicitly address how to fully utilize verification and interpretation results, which should greatly aid DRL safety. Therefore, our main contribution is an efficient method to integrate verification interpretation and learning, leveraging insights from verification and interpretation results. Through open access implementation, we aim to encourage more DRL system designers to train verifiable, interpretable safe models.

## Limitations and Conclusion

For multi-step properties, *Reinfier* itself cannot address stochasticity or unknown environments as related works (Eliyahu et al. 2021; Amir, Schapira, and Katz 2021; Ivanov et al. 2021; Jin et al. 2022), which might limit its application scenarios; the former can be alleviated through over-approximation (Clarke et al. 2000), while the latter can be addressed by environment modeling; and the lengthy verification time necessitates the improvement of verification techniques, like incremental verification. Besides, the current integration with reward shaping proves effective for simpler properties but might fall short for more intricate ones, thus integrating our framework with constrained optimization-based algorithms could enhance performance.

We present a verification-driven interpretation-in-the-loop framework *Reintrainer*, which can develop trustworthy DRL systems through property learning with verification guarantees and interpretability, without performance penalties. Additionally, we propose a general DRL verifier and interpreter *Reinfier* featuring *breakpoints* searching and *breakpoints*-based interpretation, and the language DRLP. Evaluations indicate that *Reintrainer* surpasses the SOTA across six public benchmarks, achieving superior performance and property guarantees, while *Reinfier* can verify properties and provide insightful interpretability answers.



## References

- Achiam, J.; Held, D.; Tamar, A.; and Abbeel, P. 2017. Constrained policy optimization. In *International conference on machine learning*, 22–31. PMLR.
- Amir, G.; Corsi, D.; Yerushalmi, R.; Marzari, L.; Harel, D.; Farinelli, A.; and Katz, G. 2023. Verifying learning-based robotic navigation systems. In *International Conference on Tools and Algorithms for the Construction and Analysis of Systems*, 607–627. Springer.
- Amir, G.; Schapira, M.; and Katz, G. 2021. Towards Scalable Verification of Deep Reinforcement Learning. In *2021 Formal Methods in Computer Aided Design (FMCAD)*, 193–203. IEEE. ISBN 3854480466.
- Baier, C.; and Katoen, J.-P. 2008. *Principles of model checking*. MIT press. ISBN 0262304031.
- Barto, A. G.; Sutton, R. S.; and Anderson, C. W. 1983. Neuronlike adaptive elements that can solve difficult learning control problems. *IEEE Transactions on Systems, Man, and Cybernetics*, SMC-13(5): 834–846.
- Brockman, G.; Cheung, V.; Pettersson, L.; Schneider, J.; Schulman, J.; Tang, J.; and Zaremba, W. 2016. OpenAI Gym. .
- Clarke, E.; Fehnker, A.; Han, Z.; Krogh, B.; Ouaknine, J.; Stursberg, O.; and Theobald, M. 2003. Abstraction and counterexample-guided refinement in model checking of hybrid systems. *International journal of foundations of computer science*, 14(04): 583–604.
- Clarke, E.; Grumberg, O.; Jha, S.; Lu, Y.; and Veith, H. 2000. Counterexample-guided abstraction refinement. In *Computer Aided Verification: 12th International Conference, CAV 2000, Chicago, IL, USA, July 15-19, 2000. Proceedings 12*, 154–169. Springer.
- Datta, A.; Fredrikson, M.; Leino, K.; Lu, K.; Sen, S.; and Wang, Z. 2021. Machine learning explainability and robustness: connected at the hip. In *Proceedings of the 27th ACM SIGKDD Conference on Knowledge Discovery & Data Mining*, 4035–4036.
- Dethise, A.; Canini, M.; and Kandula, S. 2019. Cracking open the black box: What observations can tell us about reinforcement learning agents. In *Proceedings of the 2019 Workshop on Network Meets AI & ML*, 29–36.
- Eliyahu, T.; Kazak, Y.; Katz, G.; and Schapira, M. 2021. Verifying learning-augmented systems. In *Proceedings of the 2021 ACM SIGCOMM 2021 Conference*, 305–318.
- Gallestey, E.; and Hokayem, P. 2019. Lecture notes in Nonlinear Systems and Control.
- Gross, D.; Jansen, N.; Junges, S.; and Pérez, G. A. 2022. COOLMC: a comprehensive tool for reinforcement learning and model checking. In *International Symposium on Dependable Software Engineering: Theories, Tools, and Applications*, 41–49. Springer.
- Guidotti, R.; Monreale, A.; Ruggieri, S.; Turini, F.; Giannotti, F.; and Pedreschi, D. 2018. A survey of methods for explaining black box models. *ACM computing surveys (CSUR)*, 51(5): 1–42.
- Hasanbeig, M.; Kroening, D.; and Abate, A. 2020. Towards verifiable and safe model-free reinforcement learning. In *CEUR Workshop Proceedings 2020*. CEUR Workshop Proceedings.
- Huang, Y.; Lin, Y.; Du, H.; Chen, Y.; Song, H.; Kong, L.; Xiang, Q.; Li, Q.; Le, F.; and Shu, J. 2023. Toward a Unified Framework for Verifying and Interpreting Learning-Based Networking Systems. In *2023 IEEE/ACM 31st International Symposium on Quality of Service (IWQoS)*, 01–10. IEEE.
- Ivanov, R.; Carpenter, T.; Weimer, J.; Alur, R.; Pappas, G.; and Lee, I. 2021. Verisig 2.0: Verification of neural network controllers using taylor model preconditioning. In *International Conference on Computer Aided Verification*, 249–262. Springer.
- Jankovic, M.; Fontaine, D.; and Kokotović, P. V. 1996. TORA example: cascade-and passivity-based control designs. *IEEE Transactions on Control Systems Technology*, 4(3): 292–297.
- Jay, N.; Rotman, N.; Godfrey, B.; Schapira, M.; and Tamar, A. 2019. A deep reinforcement learning perspective on internet congestion control. In *International Conference on Machine Learning*, 3050–3059. PMLR. ISBN 2640-3498.
- Jiaming Ji, B. Z. J. D. X. P. R. S. W. H. Y. G. M. L. Y. Y., Jiayi Zhou. 2023. OmniSafe: An Infrastructure for Accelerating Safe Reinforcement Learning Research. *arXiv preprint arXiv:2305.09304*.
- Jin, P.; Tian, J.; Zhi, D.; Wen, X.; and Zhang, M. 2022. Trainify: A cegar-driven training and verification framework for safe deep reinforcement learning. In *International Conference on Computer Aided Verification*, 193–218. Springer.
- Katz, G.; Barrett, C.; Dill, D. L.; Julian, K.; and Kochenderfer, M. J. 2017. Reluplex: An efficient SMT solver for verifying deep neural networks. In *International conference on computer aided verification*, 97–117. Springer.
- Katz, G.; Huang, D. A.; Ibeling, D.; Julian, K.; Lazarus, C.; Lim, R.; Shah, P.; Thakoor, S.; Wu, H.; and Zeljić, A. 2019. The marabou framework for verification and analysis of deep neural networks. In *International Conference on Computer Aided Verification*, 443–452. Springer.
- Kazak, Y.; Barrett, C.; Katz, G.; and Schapira, M. 2019. Verifying deep-RL-driven systems. In *Proceedings of the 2019 workshop on network meets AI & ML*, 83–89.
- Landers, M.; and Doryab, A. 2023. Deep Reinforcement Learning Verification: A Survey. *ACM Computing Surveys*.
- Lee, C.; and Landgrebe, D. A. 1997. Decision boundary feature extraction for neural networks. *IEEE Transactions on Neural Networks*, 8(1): 75–83.
- Lillicrap, T. P.; Hunt, J. J.; Pritzel, A.; Heess, N.; Erez, T.; Tassa, Y.; Silver, D.; and Wierstra, D. 2015. Continuous control with deep reinforcement learning. *arXiv preprint arXiv:1509.02971*.
- Luong, N. C.; Hoang, D. T.; Gong, S.; Niyato, D.; Wang, P.; Liang, Y.-C.; and Kim, D. I. 2019. Applications of deep reinforcement learning in communications and networking: A survey. *IEEE Communications Surveys & Tutorials*, 21(4): 3133–3174.
- Madry, A.; Makelev, A.; Schmidt, L.; Tsipras, D.; and Vladu, A. 2017. Towards deep learning models resistant to adversarial attacks. *arXiv preprint arXiv:1706.06083*.
- Meng, Z.; Wang, M.; Bai, J.; Xu, M.; Mao, H.; and Hu, H. 2020. Interpreting deep learning-based networking systems. In *Proceedings of the Annual conference of the ACM Special Interest Group on Data Communication on the applications, technologies, architectures, and protocols for computer communication*, 154–171.
- Mnih, V.; Kavukcuoglu, K.; Silver, D.; Graves, A.; Antonoglou, I.; Wierstra, D.; and Riedmiller, M. 2013. Playing atari with deep reinforcement learning. *arXiv preprint arXiv:1312.5602*.
- Molnar, C. 2020. *Interpretable machine learning*. Lulu. com.
- Moore, A. W. 1990. Efficient Memory-based Learning for Robot Control. Technical report, University of Cambridge.
- Ng, A. Y.; Harada, D.; and Russell, S. J. 1999. Policy Invariance Under Reward Transformations: Theory and Application to Reward Shaping. In *Proceedings of the Sixteenth International Conference on Machine Learning, ICML '99*, 278–287. San Francisco, CA, USA: Morgan Kaufmann Publishers Inc. ISBN 1558606122.



Nilsson, P.; Hussien, O.; Balkan, A.; Chen, Y.; Ames, A. D.; Grizzle, J. W.; Ozay, N.; Peng, H.; and Tabuada, P. 2015. Correct-by-construction adaptive cruise control: Two approaches. *IEEE Transactions on Control Systems Technology*, 24(4): 1294–1307.

Ohn-Bar, E.; and Trivedi, M. M. 2016. Looking at humans in the age of self-driving and highly automated vehicles. *IEEE Transactions on Intelligent Vehicles*, 1(1): 90–104.

Raffin, A.; Hill, A.; Gleave, A.; Kanervisto, A.; Ernestus, M.; and Dormann, N. 2021. Stable-Baselines3: Reliable Reinforcement Learning Implementations. *Journal of Machine Learning Research*, 22(268): 1–8.

Ray, A.; Achiam, J.; and Amodei, D. 2019. Benchmarking safe exploration in deep reinforcement learning. *arXiv preprint arXiv:1910.01708*, 7(1): 2.

Schulman, J.; Wolski, F.; Dhariwal, P.; Radford, A.; and Klimov, O. 2017. Proximal policy optimization algorithms. *arXiv preprint arXiv:1707.06347*.

Shriver, D.; Elbaum, S.; and Dwyer, M. B. 2022. DNNV: A Framework for Deep Neural Network Verification. In *Computer Aided Verification: 33rd International Conference, Computer Aided Verification*, 137–150. Springer International Publishing. ISBN 978-3-030-81685-8.

Silver, D.; Huang, A.; Maddison, C. J.; Guez, A.; Sifre, L.; Van Den Driessche, G.; Schrittwieser, J.; Antonoglou, I.; Panneershelvam, V.; and Lanctot, M. 2016. Mastering the game of Go with deep neural networks and tree search. *Nature*, 529(7587): 484–489.

Srinivasan, K.; Eysenbach, B.; Ha, S.; Tan, J.; and Finn, C. 2020. Learning to be safe: Deep rl with a safety critic. *arXiv preprint arXiv:2010.14603*.

Wachter, S.; Mittelstadt, B.; and Russell, C. 2017. Counterfactual explanations without opening the black box: Automated decisions and the GDPR. *Harv. JL & Tech.*, 31: 841.

Wang, Z.; Fredrikson, M.; and Datta, A. 2021. Robust models are more interpretable because attributions look normal. *arXiv preprint arXiv:2103.11257*.

Xie, C.; Wu, Y.; Maaten, L. v. d.; Yuille, A. L.; and He, K. 2019. Feature denoising for improving adversarial robustness. In *Proceedings of the IEEE/CVF conference on computer vision and pattern recognition*, 501–509.

Yang, L.; Ji, J.; Dai, J.; Zhang, L.; Zhou, B.; Li, P.; Yang, Y.; and Pan, G. 2022. Constrained update projection approach to safe policy optimization. *Advances in Neural Information Processing Systems*, 35: 9111–9124.

Yang, T.-Y.; Rosca, J.; Narasimhan, K.; and Ramadge, P. J. 2020. Projection-based constrained policy optimization. *arXiv preprint arXiv:2010.03152*.

Zhang, Y.; Tiño, P.; Leonardis, A.; and Tang, K. 2021. A survey on neural network interpretability. *IEEE Transactions on Emerging Topics in Computational Intelligence*, 5(5): 726–742.

Zhang, Z.; Xue, Z.; Chen, Y.; Liu, S.; Zhang, Y.; Liu, J.; and Zhang, M. 2023. Boosting Verified Training for Robust Image Classifications via Abstraction. In *Proceedings of the IEEE/CVF Conference on Computer Vision and Pattern Recognition*, 16251–16260.

## A Theoretical Proofs

### A.1 Theorem 1 with Proof

**Definition 1.** Property  $\dot{\phi}$  is a relaxation of property  $\phi$ , if and only if  $\phi \Rightarrow \dot{\phi}$ .

**Theorem 1.** Property  $\dot{\phi} \equiv \dot{P} \Rightarrow \dot{Q}$  is a relaxation of property  $\phi \equiv P \Rightarrow Q$ , if  $\dot{P} \subseteq P, \dot{Q} \supseteq Q$ .

*Proof.*  $\phi \Rightarrow \dot{\phi}$  means that if  $P \Rightarrow Q$ , then  $\dot{P} \Rightarrow \dot{Q}$  must also hold.

1. **Assume  $P \Rightarrow Q$ :**

By the definition of  $\phi$ , this means that for all  $x$ , if  $x \in P$ , then  $x \in Q$ .

2. **Consider  $\dot{P} \subseteq P$ :**

By this inclusion, if  $x \in \dot{P}$ , then  $x \in P$ .

3. **Using the assumption  $P \Rightarrow Q$ :**

Given that  $\dot{P} \subseteq P$ , if  $x \in \dot{P}$ , then  $x \in P$ . By the implication  $P \Rightarrow Q$ , if  $x \in P$ , then  $x \in Q$ . Hence, if  $x \in \dot{P}$ , then  $x \in Q$ .

4. **Consider  $\dot{Q} \supseteq Q$ :**

By this inclusion, if  $x \in Q$ , then  $x \in \dot{Q}$ .

5. **Combining the above steps:**

Since if  $x \in \dot{P}$ , then  $x \in P$ , and if  $x \in P$ , then  $x \in Q$ , and finally, if  $x \in Q$ , then  $x \in \dot{Q}$ . Therefore, if  $x \in \dot{P}$ , then  $x \in \dot{Q}$ .

Thus, we have shown that if  $\phi \equiv P \Rightarrow Q$  holds, then  $\dot{\phi} \equiv \dot{P} \Rightarrow \dot{Q}$  also holds. Therefore,  $\phi \Rightarrow \dot{\phi}$ , proving that  $\dot{\phi}$  is a relaxation of  $\phi$ .  $\square$

### A.2 Theorem 1 with Proof

**Definition 2.** A shaping reward function  $F : S \times A \times S \rightarrow \mathbb{R}$  is **potential-based** if there exists potential function  $\psi : S \rightarrow \mathbb{R}$  such that

$$F(s, a, s') = \gamma\psi(s') - \psi(s)$$

for all  $s \neq s_0, a, s'$ . (Ng, Harada, and Russell 1999)

**Theorem 2.** If  $F$  is a potential-based shaping function, then every optimal policy in  $M' = \langle S, A, T, \gamma, r + F \rangle$  will also be an optimal policy in  $M = \langle S, A, T, \gamma, r \rangle$  and vice versa. (Ng, Harada, and Russell 1999)

*Proof.* The optimal  $Q$ -function  $Q_M^*(s, a) = \sup_{\pi} Q_M^{\pi}(s, a)$ .  $Q_M^*$  satisfies the Bellman equation:

$$Q_M^*(s, a) = \mathbb{E}_{s' \sim P(\cdot|s, a)} \left[ R(s, a, s') + \gamma \max_{a' \in A} Q_M^*(s', a') \right]$$

Let's subtract  $\psi(s)$  from both sides:

$$\begin{aligned} & Q_M(s, a) - \psi(s) \\ &= \mathbb{E}_{s' \sim P(\cdot|s, a)} \left[ R(s, a, s') + \gamma \max_{a' \in A} Q_M^*(s', a') \right] - \psi(s) \\ &= \mathbb{E}_{s' \sim P(\cdot|s, a)} \left[ R(s, a, s') + \gamma\psi(s') + \right. \\ & \quad \left. \gamma \max_{a' \in A} (Q_M^*(s', a') - \psi(s')) \right] - \psi(s) \\ &= \mathbb{E}_{s' \sim P(\cdot|s, a)} \left[ R(s, a, s') + \gamma\psi(s') - \right. \\ & \quad \left. \psi(s) + \gamma \max_{a' \in A} (Q_M^*(s', a') - \psi(s')) \right] \end{aligned}$$

Let

$$\hat{Q}_{M'}(s, a) := Q_M^*(s, a) - \psi(s).$$

and recall that

$$F(s, a, s') = \gamma\psi(s') - \psi(s).$$

Therefore,

$$\begin{aligned} & \hat{Q}_{M'}(s, a) \\ &= \mathbb{E}_{s' \sim P(\cdot|s, a)} \left[ r(s, a, s') + F(s, a, s') + \right. \\ & \quad \left. \gamma \max_{a' \in A} (\hat{Q}_{M'}(s', a')) \right] \\ &= \mathbb{E}_{s' \sim P(\cdot|s, a)} \left[ r'(s, a, s') + \gamma \max_{a' \in A} (\hat{Q}_{M'}(s', a')) \right] \end{aligned}$$

This is the Bellman equation for  $M'$ , so

$$\hat{Q}_{M'} = Q_{M'}^*.$$

$\square$

**Corollary 1.**  $\tilde{F}_t$  does not affect the optimality of the policy.

*Proof.* Recall that

$$Diff(\phi, \mathbf{s}, \mathbf{a}) = \pm Dist(\phi, \mathbf{s}) \times Dist(\phi[\mathbf{a}], \mathbf{a})$$

$$F_t = Lr(g(\phi, N)) \times Diff(\phi, \mathbf{s}, \mathbf{a})$$

Considering the violation condition, therefore,

$$F_t = -Lr(g(\phi, N)) \times Dist(\phi, \mathbf{s}) \times Dist(\phi[\mathbf{a}], \mathbf{a})$$

For the vast majority of cases,  $Dist(\phi[\mathbf{a}], \mathbf{a})$  is set to a fixed value, and within one Reintrainer iteration,  $Lr(g(\phi, N))$  keeps unchanged. Therefore,

$$F_t = \kappa Dist_{\phi}(s)$$

So,  $F_t$  can be considered as a potential value  $\psi(s)$ .

Recall that, for destination reach property,

$$\begin{aligned} \tilde{F}_t &= \lambda F_{t+1} - F_t + \mu \tilde{F}_{t+1} \\ &= [\lambda\psi(s_{t+1}) - \psi(s_t)] + \mu \tilde{F}_{t+1} \end{aligned}$$

Generally,  $\mu$  enhances property learning based on the discount factor  $\gamma$  and typically takes on a smaller value. Therefore,

$$\tilde{F}_t \approx \lambda\psi(s_{t+1}) - \psi(s_t)$$

This is equivalent to the potential-based shaping reward function.

Recall that, for action avoiding property,

$$\tilde{F}_t = F_{t+1} - \lambda^{-1}F_{t-1} + \mu\tilde{F}_{t+1}$$

The significant difference between this and the destination reach property lies in the fact that  $F_t$  is shifted forward by one timestep. This is because, in the destination reach property, if an undesirable state region is entered at  $t + 1$ , it indicates that  $a_{t+1}$  is a bad action, and correspondingly,  $\psi(s_{t+1})$  will be smaller. However, in the action avoiding property, we consider the current state at  $t$  itself to be undesirable, indicating that  $a_t$  is a bad action. So, we shift forward by one timestep on the basis of  $\lambda F_{t+1} - F_t$  to  $F_t - \lambda^{-1}F_t$ , and they are equivalent.

Therefore, according to **Theorem 2**,  $\tilde{F}_t$  does not affect the optimality of the policy.  $\square$

## B Supplementary Details of DRLP

### B.1 Motivation

The novel DRLP appears because existing methods to encode properties, interpretability questions, and constraints aren't user-friendly. While SMT and ACTL formulas are common, they resemble pseudocodes more than programming languages. Inspired by Python's popularity in DRL, we use its syntax to encode SMT formulas more intuitively with syntactic sugars, enhancing ease of writing. In previous works, Trainify (Jin et al. 2022) claims ACTL use, but uses hardcoded conditional statements without parsing ACTL actually; model-checking approaches like whiRL (Eliyahu et al. 2021; Amir, Schapira, and Katz 2021) use DNN verifiers' API, unsuitable for DRL verification. Verisig (Kazak et al. 2019; Ivanov et al. 2021) uses hybrid system models which lack readability.

### B.2 DRLP Syntax

We design a Python-embedded Domain-Specific Language named DRLP (Deep Reinforcement Learning Property) and implement its parser. Its currently supported syntax is defined in Backus-Naur Form as:

```

1 <drlp> ::=
2   (<statements> NEWLINE '@Pre' NEWLINE)
3   <io_size_assign> NEWLINE <statements> NEWLINE
4   '@Exp' NEWLINE <statements>
5
6 <io_size_assign> ::= ''
7   | <io_size_assign> NEWLINE <io_size_id> '=' <int>
8
9 <io_size_id> ::= 'x_size' | 'y_size'
10
11 <statements> ::= ''
12   | <statements> NEWLINE <statement>
13
14 <statement> ::= <compound_stmt> | <simple_stmts>
15
16 <compound_stmt> ::= <for_stmt> | <with_stmt>
17
18 <for_stmt> ::=
19   'for' <id> 'in' <range_type> <for_range> ':'

```

```

20   <block>
21
22 <with_stmt> ::= 'with' <range_type> ':' <block>
23
24 <block> ::= NEWLINE INDENT <statements> DEDENT
25   | <simple_stmts>
26
27 <range_type> ::= 'range' | 'orange'
28
29 <for_range> ::= '(' <int> ')'
30   | '(' <int> ',' <int> ')'
31   | '(' <int> ',' <int> ',' <int> ')'
32
33 <simple_stmts> ::= ''
34   | <simple_stmts> NEWLINE <simple_stmt>
35
36 <simple_stmt> ::= <call_stmt> | <expr>
37
38 <call_stmt> ::= 'Impiles' '(' <expr> ',' <expr> ')'
39   | 'And' '(' <exprs> ')'
40   | 'Or' '(' <exprs> ')'
41
42 <exprs> ::= <expr>
43   | <exprs> ',' <expr>
44
45 <expr> ::= <obj> <comparation>
46
47 <comparation> ::= ''
48   | <comparator> <obj> <comparation>
49
50 <obj> ::= <constraint> | <io_obj>
51
52 <io_obj> ::= <io_id>
53   | <io_id> <subscript>
54   | <io_id> <subscript> <subscript>
55
56 <io_id> ::= 'x' | 'y'
57
58 <subscript> ::= '[' <int> ']'
59   | '[' <int> ':' <int> ']'
60   | '[' <int> ':' <int> ':' <int> ']'
61
62 <int> ::= <int_number>
63   | <id>
64   | <int> <operator> <int>
65
66 <constraint> ::= <int>
67   | <list>
68   | <constraint> <operator> <constraint>

```

### B.3 DRLP Design

**DRLP Structure.** A DRLP script is structured into three segments: *drlp\_v* encompassing pre-assigned variables and Python codes to execute, *drlp\_p* comprising the pre-condition  $P$  initiated by the delimiter @Pre, and *drlp\_q* comprising the post-condition  $Q$  initiated by the delimiter @Exp.

In *drlp\_v*, the statements are not directly associated with a specific property, but they facilitate to *batch verification*. Their execution outcomes, encompassing all variable values within the local scope, are transferred to the subsequent two segments for the assignment of variables without concrete values. Variables prefixed with “\_” are *iterable vari-*

ables; Cartesian products of all textsliterable variables are generated by removing “\_” from their names. To illustrate, if `a=1, _b=[2, 3], _c=[4, 5]` is in `drlp.v`, four variable values are passed to `drlp.p` and `drlp.q`:  $a = 1, b = 2, c = 4$ ;  $a = 1, b = 2, c = 5$ ;  $a = 1, b = 3, c = 4$ ;  $a = 1, b = 3, c = 5$ . Consequently, a single property in DRLP can be translated into four distinct properties, each with specific concrete values.

In `drlp.p`, it is imperative to state all pre-condition constraints. In situations where the size of the DNN input or output cannot be inferred from other statements, an explicit declaration is mandated. For instance, `x_size=3` or `y_size=1` must be clearly stated.

In `drlp.q`, all post-condition constraints are stated.

**DRLP Variables Access.** In DRLP, the input  $x$  is treated as a matrix of dimensions  $k \times n$ , where each row represents a set of inputs for the original DNN with a size of  $1 \times n$ . Similarly, the output  $y$  follows a similar structure. Slicing can be applied to access specific portions of  $x$  and  $y$ . For instance, `x[0][0:2]` refers to the 0-th and 1-st input variables of the 0-th original DNN. Also, `y[1]` denotes the output of the 1-st original DNN.

**DRLP Statement.** The statements in `drlp.p` and `drlp.q` primarily consist of constraints formulated as comparison expressions. For example, given an original DNN with an input size  $1 \times 2$ , where the initial state condition  $I$  dictates that both input variables are set to 0, this can be stated as `[0]*2 ≤ x[0] ≤ [0]*2` or `[0]*2 == x[0]`. Here, `[0]*2` is a simplified form of `[0, 0]`.

**DRLP Relation Domain.** The relation *And* is the predominant Boolean operator employed in DRL properties. As a result, the constraint statements in each line of DRLP scripts are inherently connected using the *And* relation by default. This default connection is referred to as the *And* relation domain (*range*). Consequently, the constraint statements present within this range must be simultaneously satisfied.

When certain constraints are connected by the relation *Or*, it is necessary to explicitly define the *Or* relation domain (*orange*) using the statement with `with orange:`. This signifies that within the *orange* segment, it is sufficient for just one constraint to be satisfied.

**DRLP Loop.** In DRL, it is common for certain constraints to take on similar forms due to multiple interactions. To accommodate this, DRLP introduces the `for` keyword, allowing the declaration of loop code segments in a Python-style manner. A looping range can be stated as `for i in range(0, 3) :`, similar to Python loops. Within each unrolled loop, statement segments are connected using the *And* relations.

Looping *orange* can be stated like `for i in orange(0, 3) :`, and statement segments of each unrolled loop are connected with the *Or* relation. Note that only these segments are in *orange* between them, but the statements inside a segment are still in *range* if without explicit declaration.

## C Supplementary Design of Reinifier

### C.1 DNN Adapter

Due to the multiple interactions between the agent and the environment, all constraints from the property, the DRL system, and the DNN need encoding to be consistent with verification depth  $k$  for model checking algorithms. Therefore, the agent DNN should be unrolled and encoded  $k$  times larger than the original when the verification depth is  $k$ . This unrolled DNN is used as the input DNN for DNN verification.  $x_i^j$  denotes the  $j$ -th value of the input of the  $i$ -th original DNN; the input of the  $i$ -th original DNN  $x_i$  is  $\langle x_i^0, \dots, x_i^{n-1} \rangle$ ; the input  $x$   $\langle x_0, \dots, x_{k-1} \rangle$ .  $y_i^j$  denotes the  $j$ -th value of the output of the  $i$ -th original DNN; the output of the  $i$ -th original DNN  $y_i$  is  $\langle y_i^0, \dots, y_i^{m-1} \rangle$ ; the output  $y$  is  $\langle y_0, \dots, y_{k-1} \rangle$ .

### C.2 Type of Properties

All constraints from the property and the DRL system need encoding. Thus, pre-condition  $P$  can be divided into the following four parts:

(i) **State boundary condition  $S$** : describes the boundary of the environment in DRL, and all input features should be bounded. (ii) **Initial state condition  $I$** : describes the initial state of the system, because a DRL system could start from a defined state or within a particular state boundary. (iii) **State transition condition  $T$** : describes how the environment transits from the current state  $x_i$  to the new state  $x_{i+1}$ . Generally, the action  $N(x_i)$  taken by the agent plays a pivotal role in the state transition, but  $x_{i+1}$  is not only determined by  $N(x_i)$  but also affected by random factors. (iv) **Other condition  $C$** : describes extra constraints related to specified properties. It stands apart from the  $S$ ,  $I$ , and  $T$  parts, which usually describe the unchanging characteristics of a particular DRL system. For example, liveness properties (Baier and Katoen 2008) require no state cycle existing, such as  $x_0! = x_2$ ; and this constraint should be considered as an extra constraint due to its exclusive association with this particular property, rather than being a characteristic of the entire system. We believe that distinct division in this way is beneficial for users to formulate and articulate properties.

**Post-condition  $S$** : describes the expected result of a given DRL system under previous constraints.

Safety properties (Baier and Katoen 2008) represent one of the paramount property types, where the agent is expected to persistently avoid undesirable actions under given pre-conditions. Safety properties guarantee that the DRL system will never transition into *bad* states. The predicate  $Good(N(x))$  evaluates as `True` when in *good* states and vice versa. Such a property is formulated as:

$$\begin{aligned} \forall x_0, x_1, \dots, \bigwedge_{i=0} (S(x_i) \wedge I(x_i) \wedge T(x_i, x_{i+1}) \wedge C(x_i)) \\ \Rightarrow \bigwedge_{i=0} (Good(N(x_i))) \end{aligned} \quad (8)$$

Another type of property is liveness property (Baier and Katoen 2008), where the agent might take undesirable actions but is expected to eventually take desirable ones. Liveness properties guarantee that the DRL system will not re-

main persistently trapped in *bad* states. Thus, verifying liveness properties involves the optional detection of cycles of states consistently in *bad* states.  $C'(x)$  denotes  $C(x)$  without cycle detection, i.e.,  $x_i! = x_\gamma$ . Such a property is formulated as:

$$\forall x_0, x_1, \dots, \bigwedge_{i=0} (S(x_i) \wedge I(x_i) \wedge T(x_i) \wedge C'(x_i) \wedge (\bigwedge_{\gamma=0}^{i-1} (x_i! = x_\gamma))) \Rightarrow \bigvee_{i=0} (Good(N(x_i))) \quad (9)$$

Robustness properties assess the stability of the agent’s performance within adversarial environments, which constrains the agent to take consistent or similar actions in the presence of perturbed input values (local robustness (Datta et al. 2021)) or input outliers (extreme value robustness (Katz et al. 2017)).  $\hat{x}_0$  denotes the original input, and  $\varepsilon$  denotes perturbation. Such a property is formulated as:

$$\forall x_0, I(x_0) \wedge C(x_0) \Rightarrow N(x_0) \approx N(\hat{x}_0) \quad (10)$$

For local robustness,  $I(x_0) \equiv \bigwedge_{i=0} (\hat{x}_0^i - \varepsilon^i \leq x_0^i \leq \hat{x}_0^i + \varepsilon^i)$ ; for extreme value robustness,  $I(x_0) \equiv \bigwedge_{i \in D} (\hat{x}_0^i - \varepsilon^i \leq x_0^i \leq \hat{x}_0^i + \varepsilon^i) \wedge \bigwedge_{i \in R} (\hat{x}_0^i - \varepsilon^i \leq x_0^i \leq \hat{x}_0^i + \varepsilon^i)$ , in which  $D$  denotes the set of indices of the input features whose values are outliers, while  $R$  denotes the set of indices of other input features.

### C.3 Single Verifier

**C.3.1 Model Checking Algorithm.** Inspired by related works (Eliyahu et al. 2021; Amir, Schapira, and Katz 2021), we implement the following algorithms in Single Verifier.

**Bounded model checking (BMC).** As the verification depth  $k$  increases from 1, both the original DNN and the DRLP script are unrolled or translated with depth  $k$ . Then, DNN verifier is queried. The query is formulated as:

$$\forall x_0, \dots, x_{k-1}, (\bigwedge_{i=0}^{k-1} (S(x_i) \wedge C(x_i))) \wedge I(x_0) \wedge (\bigwedge_{i=0}^{k-2} T(x_i, x_{i+1})) \rightarrow \bigwedge_{i=0}^{k-1} Q((N(x_i))) \quad (11)$$

**$k$ -induction.** The first phase of  $k$ -induction, the basic situation verification, is identical to the BMC process; while the second phase diverges. In the inductive hypothesis verification, the original DNN is unrolled with depth  $k + 1$ , and the DRLP script is translated for indication verification with depth  $k + 1$  and an assumption that the property holds with depth  $k$ . Then, the DNN verifier is queried. The query is for-

mulated as:

$$\forall x_\alpha, \dots, x_{\alpha+k}, (\bigwedge_{i=\alpha}^{\alpha+k} (S(x_i) \wedge C(x_i))) \wedge (\bigwedge_{i=\alpha}^{\alpha+k-1} (T(x_i, x_{i+1}) \wedge Q(N(x_i)))) \rightarrow Q(N(x_{\alpha+k})) \quad (12)$$

**C.3.2 Reachability Analysis** Through our DRLP parser and DNN adapter, we use Verisig (Ivanov et al. 2021) for reachability analysis.

### C.4 Batch Verifier

---

#### Algorithm 2: FindBreakpoints (General Form)

---

**Input:** DRLP template  $p$ , DNN  $N$ , variable list  $\{vars\}$

**Output:** Breakpoint list  $\{bp\}$

```

1:  $var \leftarrow$  pop the top variable from  $\{vars\}$ 
2:  $lb \leftarrow$  the lower bound of  $var$ ,  $ub \leftarrow$  the upper bound of  $var$ 
3:  $prec \leftarrow$  the search precision of  $var$ 
4:
5: while TRUE do
6:    $lb, ub, curr \leftarrow$  step( $lb, ub, curr, prec, p, N, var, \{vars\}$ )
7:   if  $curr = \text{None}$  then
8:     break
9:   end if
10:   $script \leftarrow$  concretize( $p, var, curr$ )
11:  if  $\{vars\}$  is empty then
12:     $curr_r, violation \leftarrow$  verify( $script, N$ )
13:    if  $curr_r \neq prev_r$  then
14:      Add  $script$ ’s corresponding property to  $\{bp\}$ 
15:    end if
16:     $prev_r \leftarrow curr_r$ 
17:  else
18:    FindBreakpoints( $script, N, \{vars\}$ )
19:  end if
20: end while

```

---

We design Algorithm 2 to identify *breakpoints*, using three representative methods in the function *step*: linear, binary, and iterative search. The Algorithm 1 in the main text is a special case of Algorithm 2, and also the most common case, where all variables in the variable list  $\{vars\}$  are searched using linear search except for the last variable, which uses binary search.

### C.5 Interpreter

In addition to the problems in the main text, we also provide solutions to the following problems, which are similarly based on breakpoints.

**C.5.1 Decision Boundary** For a robustness property (Lee and Landgrebe 1997; Wang, Fredrikson, and Datta 2021), the data points, which are formed by the parameters extracted from the *breakpoints*, are part of the decision boundary. This perspective inspires us to discern the specific conditions under which the DRL system satisfies given safety, liveness, and robustness properties. Additionally, in the context of safety and liveness properties, if the verification depth is confined to  $k = 1$ , i.e., degenerating into one-shot DNN verification, the parameters extracted

---

**Function step**

---

**Input:** lower bound  $lb$ , upper bound  $ub$ , current value  $curr$ , search precise  $prec$ , DRLP template  $p$ , DNN  $N$ , variable  $var$ , variable list  $\{vars\}$

**Output:** lower bound  $lb$ , upper bound  $ub$ , current value  $curr$

```
1: {Linear Search}
2: if  $curr \leq ub$  then
3:    $curr \leftarrow curr + prec$ 
4: else
5:    $curr \leftarrow \text{None}$ 
6: end if
7:
8: {Binary or Iterative Search}
9:  $lb\_r, violation \leftarrow \text{verify}(\text{concretize}(p, var, lb, \{vars\}), N)$ 
10:  $ub\_r, violation \leftarrow \text{verify}(\text{concretize}(p, var, ub, \{vars\}), N)$ 
11:  $curr\_r, violation \leftarrow \text{verify}(\text{concretize}(p, var, curr, \{vars\}), N)$ 
12:    $curr\_r \leftarrow \text{the value of } var \text{ in } violation$ 
13: if  $curr\_r = \text{Falsified}$  then
14:    $curr \leftarrow \text{the value of } var \text{ in } violation$ 
15: end if
16:
17: {Binary Search}
18: if  $ub - lb > prec$  then
19:   if  $lb\_r = curr\_r$  then
20:      $lb \leftarrow curr$ 
21:   else if  $ub\_r \neq curr\_r$  then
22:      $ub \leftarrow curr$ 
23:   end if
24:    $curr \leftarrow \frac{lb+ub}{2}$ 
25: else
26:    $curr \leftarrow \text{None}$ 
27: end if
28:
29: {Iterative Search}
30: if  $lb\_r = curr\_r$  then
31:    $curr \leftarrow curr \times \text{iterative\_step}$ 
32: else
33:    $ub \leftarrow curr$ 
34:   Switch to Linear or Binary Search
35: end if
```

---

from the identified *breakpoints* are also recognized as invariants (Amir, Schapira, and Katz 2021), which indicates the boundary between conditions wherein the property always holds or never holds.

**Our solution:** Find *breakpoints* by stepping through interested parameters; and fit the corresponding decision boundary with the data points consisting of parameters extracted from these *breakpoints*.

**C.5.2 Intuitiveness Examination** An intuitive insight of the example of sending data using the computer: the worse the network condition is, the more reasonable for the computer to decrease its sending rate. When focusing on safety and liveness properties, as the values of certain parameters in the property increase or decrease, the associated constraints will consequently become more tightened or relaxed, rendering the property either easier or harder to hold; and this idea leads us to propose the intuitiveness examination.

**Our solution:** Find *breakpoints* by linear stepping through interested parameters; and if the count of the identified *breakpoints* is either 0 or 1, the intuitiveness examination passes.  $\{bp\}$  denotes the list of corresponding properties associated with identified *breakpoints*, and the answer to this question is formulated as:  $|\{bp\}| \in \{0, 1\}$ .

**C.5.3 Counterfactual Explanation** Given the original input  $\hat{x}_0$  and the target counterfactual output  $\hat{y}_0$  such that  $\hat{y}_0 \not\approx N(\hat{x}_0)$ , the counterfactual explanation question (Molnar 2020; Wachter, Mittelstadt, and Russell 2017) aims to identify the counterfactual inputs  $\{x_0\}$  such that  $N(x_0) \approx \hat{y}_0$ . The most valuable counterfactual input  $x_0$  is the one that is closest (according to vector distance) to the original input  $\hat{x}_0$ . Because the minimum vector distance often implies the minimum attack cost (Madry et al. 2017), this counterexample can effectively highlight the system’s weakness.

**Our solution:** Find *breakpoints* by stepping through possible perturbation value  $\varepsilon_0^j$  of each input  $x_0^j$  on the property formulated as:

$$\forall x_0, \bigwedge_{j=0}^{n-1} (\hat{x}_0^j - \varepsilon_0^j \leq x_0^j \leq \hat{x}_0^j + \varepsilon_0^j) \Rightarrow N(x_0) \approx \hat{y}_0 \quad (13)$$

Here, we expand the question to encompass safety and liveness properties as well: safety,  $P \equiv \bigwedge_{i=0} (\bigwedge_{j=0}^{n-1} (\hat{x}_i^j - \varepsilon_i^j \leq x_i^j \leq \hat{x}_i^j + \varepsilon_i^j)) \wedge T(x_i, x_{i+1}) \wedge I(x_0)$ ; liveness,  $P(x) \equiv \bigwedge_{i=0} ((\bigwedge_{j=0}^{n-1} (\hat{x}_i^j - \varepsilon_i^j \leq x_i^j \leq \hat{x}_i^j + \varepsilon_i^j) \wedge T(x_i, x_{i+1}) \wedge (\bigwedge_{\gamma=0}^{i-1} (x_i^\gamma = x_\gamma))) \wedge I(x_0)$ . Finally, the answer is the input closest to the original input, formulated as:  $\arg \min_{bp \in \{bp\}} d(\hat{x} + \varepsilon, \hat{x})$ , where  $d$  denoted a specific distance function.

**C.5.4 Importance Analysis** Given the original input  $\hat{x}_0$ , the importance analysis question (Guidotti et al. 2018) aims to evaluate the distances between  $x_0$  and  $\hat{x}_0$ , where  $x_0$  denotes the input whose features under discussion can be perturbed such that  $N(x_0) \not\approx N(\hat{x}_0)$ . The lower the distance, the more important the feature, as even a slight perturbation in the input of such a feature can induce greater fluctuations in the output. Importance analysis on all input features can identify which holds a central role in the decision-making process.

**Our solution:** Find *breakpoints* by stepping through possible perturbation values  $\{\varepsilon_0^j\}$  applied to the input features  $\{x_0^j\}$  on the property formulated as:

$$\forall x_0, \bigwedge_{j \in D} (\hat{x}_0^j - \varepsilon_0^j \leq x_0^j \leq \hat{x}_0^j + \varepsilon_0^j) \wedge \bigwedge_{j \in R} (\hat{x}_0^j = x_0^j) \Rightarrow N(x_0) \not\approx N(\hat{x}_0) \quad (14)$$

where  $D$  denotes the set of indices of the discussed features within the input, while  $R$  denotes the set of indices of other features. Finally, the answer is the minimum distance between  $\hat{x}_0 + \varepsilon_0$  and  $\hat{x}_0$ , i.e., importance, formulated as:  $\min_{bp \in \{bp\}} d(\hat{x}_0 + \varepsilon_0, \hat{x}_0)$ .

## D Supplementary Details of Reintrainer

### D.1 Distance of States in 1-Dimension.

To elucidate our algorithm in *Reintrainer* and our motivation, we employ the Mountain Car (Moore 1990) task as a case study. The task consists of a car placed stochastically at a valley’s bottom, and its goal is to accelerate the car to reach the top of the right hill. The agent can take one of three discrete actions: accelerate to the left, to the right, or not accelerate. The environment states consist of two features: the car’s position along the x-axis  $p$ , and the car’s velocity  $v$ .

Considering the safety property  $\phi_1$  of Mountain Car (then denoted by  $\phi$ ,  $\phi \equiv \langle p, v \rangle \in [(-0.60, 0.03), (-0.40, 0.07)] \Rightarrow \text{Action} \neq 0$ ) defined in Evaluation, if this property is violated under the conditions such as when  $\langle p, v \rangle$  is **(i)**  $\langle -0.50, 0.05 \rangle$ , **(ii)**  $\langle -0.41, 0.05 \rangle$ , **(iii)**  $\langle -0.59, 0.05 \rangle$ , **(iv)**  $\langle -0.50, 0.07 \rangle$ , the agent’s action is 0.

**Raw distance.** The agent in **(i)** should be penalized more severely than in **(ii)**, because the latter only needs to make a minor adjustment, i.e., reduce  $p$  to 0.4 to satisfy the property. Therefore, the distance from **(i)** to the boundary should be greater than the distance from **(ii)**. Therefore, we define a raw distance function: given the state feature  $s_i^j$  whose current observation is  $\mathbf{v}$ , its raw distance  $dist'$  to its property-constrained space  $\phi[s_i^j]$  in 1-dimension is formulated as:

$$dist'(\phi[s_i^j], \mathbf{v}) = \min(|\underline{\phi}[x_i^j] - \mathbf{v}|, |\bar{\phi}[x_i^j] - \mathbf{v}|) \quad (15)$$

**Distance density.** However, the raw distance measure  $dist'$  is not sufficient for certain scenarios, such as when comparing **(ii)** with **(iii)**. In both cases, the value of  $p$  is equally close to the boundary, yet the fluctuations in the output could be different for the same input feature at different values. This observation leads us to the concept of sensitivity analysis mentioned in interpretability questions, which is used to measure the potential of a feature to induce fluctuations in the output.

Given the DNN  $N$  and the original input  $\hat{x}_0$ , when the input feature  $x_0^j$  is subject to perturbation  $\varepsilon$ , the sensitivity of  $x_0^j$  can be formulated as:

$$\text{Sensitivity}(N, \hat{x}_0, x_0^j) = \max_{x_0} d(N(\hat{x}_0), N(x_0)) \quad (16)$$

where  $x_0 \in [(\hat{x}_0^0, \hat{x}_0^1, \dots, \hat{x}_0^j - \varepsilon, \dots, \hat{x}_0^{n-1}), (\hat{x}_0^0, \hat{x}_0^1, \dots, \hat{x}_0^j + \varepsilon, \dots, \hat{x}_0^{n-1})]$ .

Considering that perturbations need only be evaluated in one direction at the boundary, we define two types of *density* measures:

The first is the *density* of the lower bound  $\underline{\rho}(N, \hat{x}_0, x_0^j)$ , where  $x_0 \in [(\hat{x}_0^0, \hat{x}_0^1, \dots, \hat{x}_0^j, \dots, \hat{x}_0^{n-1}), (\hat{x}_0^0, \hat{x}_0^1, \dots, \hat{x}_0^j + \varepsilon, \dots, \hat{x}_0^{n-1})]$ . The second is the *density* of the upper bound  $\bar{\rho}(N, \hat{x}_0, x_0^j)$ , where  $x_0 \in [(\hat{x}_0^0, \hat{x}_0^1, \dots, \hat{x}_0^j - \varepsilon, \dots, \hat{x}_0^{n-1}), (\hat{x}_0^0, \hat{x}_0^1, \dots, \hat{x}_0^j, \dots, \hat{x}_0^{n-1})]$ . The function is also denoted as  $\underline{\rho}(\phi, s_i^j)$  for simplicity, as Eq. 2 in the main text.

**Exact middle point.** The exact middle point, denoted as  $\dot{\phi}[s_i^j]$ , represents the position with the maximum distance to the boundary, and also the point where the *density* of the lower and upper boundaries switch. Accordingly, this point should be closer to the boundary that exhibits greater *density*. Consequently, we determine the exact middle point by calculating the midpoint of the *density*-weighted upper and lower bounds. Besides, in the comparison between scenarios **(i)** with **(iv)**, although  $v$  in **(iv)** is closer to  $\phi[v]$ , the value of  $v$  equaling 0.07 is actually the upper bound of velocity in the Mountain Car environment (denoted by  $\bar{S}[v]$ ). Therefore, a significant adjustment is needed in **(iv)**, i.e., reduce  $v$  to 0.3 to satisfy the property. Consequently, the distance from **(iv)** to the boundary should be greater than the distance from **(i)**. Therefore, the exact middle point considering the environmental boundaries is formulated as:

$$\dot{\phi}[s_i^j] = \begin{cases} \underline{S}[s_i^j] & \text{if } \underline{\phi}[s_i^j] = \underline{S}[s_i^j] \\ & \wedge \bar{\phi}[s_i^j] \neq \bar{S}[s_i^j] \\ \frac{\underline{\rho}(\phi, s_i^j) \cdot \underline{\phi}[s_i^j] + \bar{\rho}(\phi, s_i^j) \cdot \bar{\phi}[s_i^j]}{\underline{\rho}(\phi, s_i^j) + \bar{\rho}(\phi, s_i^j)} & \text{else} \\ \bar{S}[s_i^j] & \text{if } \underline{\phi}[s_i^j] \neq \underline{S}[s_i^j] \\ & \wedge \bar{\phi}[s_i^j] = \bar{S}[s_i^j] \end{cases} \quad (17)$$

### D.2 Practical Method to Metric of Gap

One parameter  $z$  from the environment state features or the action should be chosen for the gap measure. In our implementation, *Reintrainer* could automatically choose the lower bound of action for continuous action space or the lower bound of the first environment state for discrete action space by default as the metric parameter; and it can also be chosen manually.

For example, the property  $\phi \equiv x > 0 \Rightarrow N(x) > 0$  is predefined. We choose the lower bound of action as the metric parameter. If the verifier falsifies  $\phi$ , a relaxation domain of  $\phi$  can be obtained by relaxing the action’s constraint interval according to Theorem 1. For instance, changing  $N(x) > 0$  to  $N(x) > -10$  forms  $\dot{\Phi}_{x>0 \Rightarrow N(x)>0} = \{x > 0 \Rightarrow N(x) > a : \forall a \in [-10, 0]\}$ . Using the *breakpoint* search algorithm, setting the search bounds of variable  $a$  to  $[-10, 0]$  allows us to identify the set of *breakpoint*  $\{bp\}$ , such as  $\{x > 0 \Rightarrow N(x) > -5\}$ . Then, we calculate  $g(\phi, N) = \min_{\phi \in bps} |\phi[z] - \dot{\phi}[z]| = |0 - (-5)| = 5$ . If no *breakpoint* are found, the search bounds of variable  $a$  are expanded to  $[-40, 0]$ , and the process is repeated until any *breakpoint* is found.

The method for expanding the search bounds is quite subjective. Typically, the *breakpoint* search adopts a binary stepping approach, so one possible way is to quadruple the size of the search interval each time.

### D.3 Weights for Multiple Properties

If multiple properties are simultaneously required to be satisfied, a weight  $w$  can be assigned to each property. The weights can be assigned manually based on the importance or based on the preference of each property, with higher



	$\phi_7$	$\phi_8$	$\phi_9$	$\phi_{10}$
Type	Liveness	Liveness	Safety	Liveness
State Boundary $S$	$i \in [-0.01, +0.01]$ $l \in [ 1.00, 1.01]$ $r \in [ 1.00, 1.00]$	$i \in [-0.01, +0.01]$ $l \in [ 1.00, 1.01]$ $r \in [ 1.00, 1.00]$	$i \in [-0.01, +0.01]$ $l \in [ 1.00, 1.01]$ $r \in [ 2.00, 100.00]$	$i \in [-0.01, +0.01]$ $l \in [ 1.00, 1.01]$ $r \in [ 2.00, 100.00]$
Other Condition $C$	No state cycle	No state cycle	None	No state cycle
Initial State $I$	None			
State Transition $T$	History features shift by one value			
Post-condition $Q$	Exist $N(x_i) \not\approx 0$	Exist $N(x_i) > 0$	Forall $N(x_i) < 0$	Exist $N(x_i) < 0$
Reinfier Result	Proven	Falsified	Falsified	Falsified
whiRL Result	Proven	Falsified	Falsified	Proven

Table 3: Aurora safety and liveness properties and comparison of their results by Reinfier and whiRL.

	$\phi_{11}$	$\phi_{12}$	$\phi_{13}$	$\phi_{14}$
Type	Local Robustness	Local Robustness	Extreme Value	Extreme Value
$\langle i, l, r \rangle$	$\langle 2.00, 2.00, 10.00 \rangle$	$\langle -0.70, 0.50, 1.00 \rangle$	$\langle 0.00, 1.05, 1.00 \rangle$	$\langle 0.00, 1.05, 1.00 \rangle$
Original Input $\hat{x}_0$				
Perturbation $\varepsilon$	$\langle 0.00, 0.01, 0.01 \rangle$	$\langle 0.01, 0.01, 0.00 \rangle$	$\langle 0.005, 0.005, 20 \rangle$	$\langle 0.005, 0.005, -0.05 \rangle$
Post-condition $Q$	$N(x_0) \approx N(\hat{x}_0)$ $\varepsilon = 0.05$	$N(x_0) \approx N(\hat{x}_0)$ $\varepsilon = 0.05$	$N(x_0) \approx N(\hat{x}_0)$ $\varepsilon = 1.0$	$N(x_0) \approx N(\hat{x}_0)$ $\varepsilon = 0.3$
Reinfier Result	Proven	Falsified	Falsified	Falsified
whiRL Result	Not applicable	Not applicable	Not applicable	Not applicable

Table 4: Aurora robustness properties and comparison of their results by Reinfier and whiRL.

weights given to properties more likely to be satisfied. Another approach is to build a decision tree based on predefined properties, with constraints of a property starting from the root node and ending at a leaf node. We believe that the deeper the leaf node, the more relaxed the property. By arranging all properties according to their depth, a sequence of properties ranging from relaxed to stringent can be established, and their weights can be chosen in ascending or descending order. We use factor  $\beta$  to scale the effect of  $\hat{F}_t^i$  as a whole, and we find during the evaluation that when intermediate reward sum  $\hat{F}_t$  and  $r_t$  are at the same order of magnitude, our approach works well. The intermediate reward sum function is formulated as:

$$\hat{F}_t = \beta \sum w^i \tilde{F}_t^i \quad (18)$$

In addition to reward shaping, each  $\tilde{F}_t^i$  can also be the cost respectively in Constrained MDP.

#### D.4 Counterexamples Generation

*Reintrainer* can actively generate a small number of counterexamples in the buffer for the agent’s property learning. Specifically, *Reintrainer* initially relies on reward shaping for property learning during training, and if few or no violations occur but the predefined properties are falsified, it later

combines reward shaping with data augmentation using generated counterexamples.

## E Supplementary Evaluation

### E.1 Reinfier

**E.1.1 Study Case** To demonstrate the usability and efficacy of *Reinfieras* well as provide some insights into the model, we opt for the study case Aurora (Jay et al. 2019) utilized in related works whiRL (Eliyahu et al. 2021; Amir, Schapira, and Katz 2021) and UIN (Huang et al. 2023) as the experimental environment.

Aurora is a DRL system for congestion control of Transmission Control Protocol (TCP). It takes the latest 10-step history of these features as input: latency inflation  $i$ , latency ratio  $l$ , send ratio  $r$ ; and it outputs the changed ratio of sending rate over the sending rate of the last action.

**E.1.2 Verification** Four properties are proposed in whiRL (Eliyahu et al. 2021; Amir, Schapira, and Katz 2021) as follows.

$\phi_7$ : When the history of local observations reflects excellent network conditions (close-to-minimum latency, no packet loss), the DNN should not get stuck at its current rate.

	<b>whiRL</b>	<b>Reinfier</b>	Benefit
Input Format	Hardcoded DNN verifier APIs & without APIs for DRL	Separate DRLP text into user-friendly APIs	Enhances reusability
Property Syntax	Syntax of the DNN verifier	Intuitive and concise DRLP syntax	Make it easy for users to read and write
DNN Structure	A small amount of structures	Almost all structures	Support more DRL systems and adapt to the rapid development of DNN
Result Guarantee	Results from a single DNN verifier	Comprehensive results from multiple DNN verifiers	Reduce the risk of verification error
Type of Property	Safety, Liveness	Safety, Liveness, Robustness	Facilitate thorough property verification

Table 5: Advantages of Reinfier compared to whiRL.

	$\phi_{9.d}$	$\phi_{7.a}$	$\phi_{11.a}$	$\phi_{12.a}$
Type	Safety	Liveness	Robustness	Robustness
Variables	$a \in [1.0, 10.0]$ $b \in [1, 100]$	$a \in [-0.70, -0.50]$ $b \in [1.0, 20.0]$	$a \in [1.5, 2.5]$ $b \in [6.0, 12.0]$	$a \in [-0.70, -0.50]$ $b \in [0.0, 5.0]$
State Boundary $S$ or Initial State $I$	$i \in [a, 100]$ $l \in [b, 100]$ $r \in [2, 100]$	$i \in [a, a]$ $l \in [b, b]$ $r \in [1, 1]$	$i \in [2.0, 2.0]$ $l \in [a - \varepsilon, a + \varepsilon]$ $r \in [b - \varepsilon, b + \varepsilon]$ $\varepsilon = 0.005$	$i \in [a - \varepsilon, a + \varepsilon]$ $l \in [b - \varepsilon, b + \varepsilon]$ $r \in [1.00, 2.00]$ $\varepsilon = 0.005$
$\langle i, l, r \rangle$ Original Input $\hat{x}_0$		None	$\langle 2.0, 2.0, 10.0 \rangle$	$\langle -0.70, 0.50, 1.00 \rangle$
Other Condition $C$	None	No state cycle	None	None
State Transition $T$	History features shift by one value			None
Post-condition $Q$	Forall $N(x_i) < 0$	Exist $N(x_i) > 0$	$N(x_0) \approx N(\hat{x}_0)$ $\epsilon = 0.5$	$N(x_0) \approx N(\hat{x}_0)$ $\epsilon = 0.5$

Table 6: Aurora decision boundary questions.

$\phi_8$ : When the history of local observations reflects excellent network conditions (close-to-minimum latency, no packet loss), the DNN should not constantly maintain or decrease its sending rate.

$\phi_9$ : When the congestion controller is sending on a link with a shallow buffer (and so experienced latency is always close to the minimum latency) and experiences high packet loss, it should decrease its sending rate.

$\phi_{10}$ : When the congestion controller is sending on a link with a shallow buffer (and so experienced latency is always close to the minimum latency) and consistently experiences high packet loss, it should not indefinitely maintain or increase its sending rate.

We verify these properties by *Reinfier* but get a different result shown in Table 3. It has been confirmed by the authors of whiRL (Eliyahu et al. 2021) that it is a mistake in their papers after our feedback.

Here, we propose four robustness properties for evaluation. These properties are subsequently verified by *Reinfier*, and the outcomes are presented in Table 4.  $\phi_{11}$  and  $\phi_{12}$

are local robustness.  $\phi_{13}$  describes a scenario where the input values of a single feature, i.e., send ratio, are extremely large; while  $\phi_{14}$  describes a scenario where the input values of a single feature, i.e., send ratio, are abnormal behavior. This abnormal behavior is unrealistic in real-world contexts because the send ratio cannot be less than 1, which implies receiving more packages than sent ones.

**Comparison.** When compared to the verification tool whiRL, our *Reinfier* possesses several advantages shown in Table 5. As demonstrated by the results for Aurora in Table 3, the error in whiRL can be attributed to the incorrect encoding of the property. This emphasizes the importance of using concise and intuitive syntax for encoding properties, which can greatly enhance the widespread and accurate application of DRL verification.

**E.1.3 Interpretation** Additionally, we apply *Reinfier* for the interpretation of Aurora in the context of the five interpretability questions outlined in the main text.

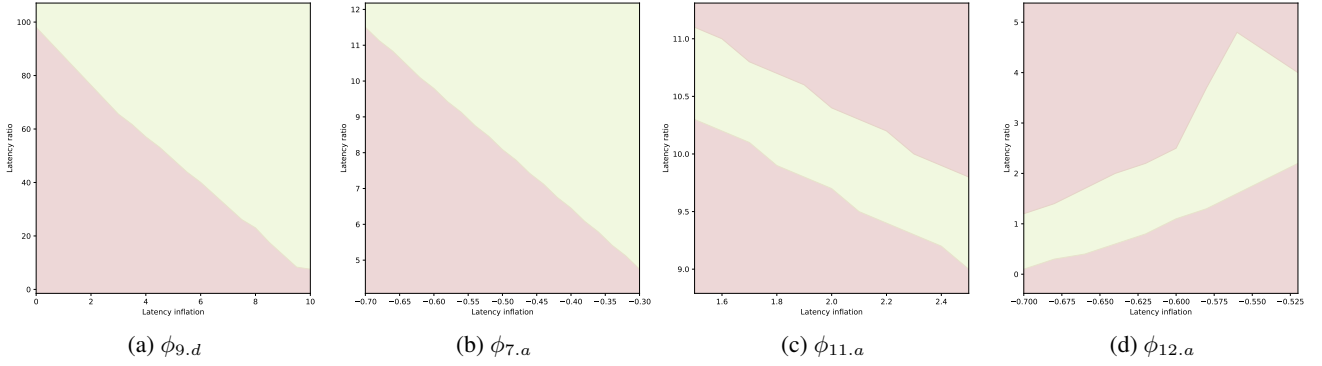


Figure 4: Aurora decision boundary. The red area represents the condition where properties do not hold, while the green area represents the condition where properties hold.

	$\phi_{10.a}$	$\phi_{9.a}$	$\phi_{9.b}$	$\phi_{9.c}$
Type	Liveness	Safety	Safety	Safety
Variable	$var \in [1, 100]$	$var \in [1, 100]$	$var \in [1, 100]$	$var \in [1, 100]$
State Boundary $S$	$i \in [-0.01, +0.01]$ $l \in [1.00, 1.01]$ $y \in [var, 100.00]$	$i \in [-0.01, +0.01]$ $l \in [1.00, 1.01]$ $y \in [var, 100.00]$	$i \in [-0.01, +0.01]$ $l \in [1.00, 1.01]$ $y \in [2.00, 100.00]$	$i \in [-0.01, +0.01]$ $l \in [var, 1.01]$ $y \in [2.00, 100.00]$
Other Condition $C$	No state cycle	None	None	None
Initial State $I$	None			
State Transition $T$	History features shift by one value			
Post-condition $Q$	Exists $N(x_i) < 0$	Forall $N(x_i) < 0$	Forall $N(x_i) < var$	Forall $N(x_i) < 0$
Breakpoint(s)	$var = 50.11$	$var = 50.11$	$var = 86$	$var = 98.07$
Reinifier Result	Proven	Proven	Proven	Proven
UINT Result	Not applicable	Not applicable	Not applicable	Not applicable

Table 7: Aurora intuitiveness examination questions and comparison of their verification results by Reinifier and UINT.

**Decision boundary.** Based on the previous properties of Aurora, we opt for one safety, one liveness, and two robustness properties to analyze their decision boundaries, detailed in Table 6. In the case of safety and liveness, the decision boundary delineates the condition where the agent takes safe or lively actions. As long as the environmental state falls within the specified space, the agent’s actions align with the desired properties, averting unforeseen bad actions.

The results shown in Fig. 4 reveal that, within the designated range, the decision boundaries for safety and liveness properties are *linear*, effectively partitioning the input space into two regions: one where the property holds and another where not. Conversely, the decision boundary for the robustness property is *coarse*, segmenting the input space into three distinct zones: a central area where the property holds, flanked by two regions where not.

**Intuitiveness examination.** Based on the previous properties of Aurora, we evaluate *Reinifier* to answer several intuitiveness examination questions, as shown in Table 7.

$\phi_{10.a}$ : This property is derived from  $\phi_{10}$ . **Qualitative property:** A higher send ratio, which implies more severe

packet loss, is associated with a greater likelihood of the sending rate eventually decreasing. The result shows that this property only has one breakpoint for  $var \in [1, 100]$  following linear stepping. Within this range, the properties transition from not holding to holding. Consequently, the model passes the intuitiveness examination on this qualitative property.

$\phi_{9.a}$ : This property is derived from  $\phi_9$ . **Qualitative property:** A higher send ratio, which implies more severe packet loss, is associated with a greater likelihood of the sending rate immediately decreasing. The result shows that this property only has one breakpoint for  $var \in [1, 100]$  following linear stepping. Consequently, the model also passes the intuitiveness examination on this qualitative property. Interestingly, in comparison to  $\phi_{4.a}$ , this result reveals that safety properties are more tightened than liveness ones for the same property structure.

$\phi_{9.b}$ : This property is derived from  $\phi_9$ . **Qualitative property:** The border the constrained range of output is, which implies the more relaxed post-condition, the higher the likelihood of the property being satisfied. The result shows that

	$\phi_{9.d}$	$\phi_{7.a}$	$\phi_{11.b}$	$\phi_{12.b}$
Type	Safety	Liveness	Robustness	Robustness
State Boundary $S$ or Initial State $I$	$i \in [0.00 + a, 100]$ $l \in [1.00 + b, 100]$ $r \in [2.00 + c, 100]$	$i \in [-0.01 - a,$ $+0.01 + a]$ $l \in [1.00 - b,$ $1.01 + b]$ $r \in [1.0 - c,$ $1.0 + c]$	$i \in [0.0 - a,$ $0.0 + a]$ $l \in [1.0 - b,$ $1.0 + b]$ $r \in [1.0 - c,$ $1.0 + c]$	$i \in [-0.7 - a,$ $-0.7 + a]$ $l \in [0.5 - b,$ $0.5 + b]$ $r \in [1.0 - c,$ $1.0 + c]$
Original Input $\hat{x}_0$		None	$\langle 2.00, 2.00, 10.00 \rangle$	$\langle -0.70, 0.50, 1.00 \rangle$
$\langle i, l, r \rangle$		None	-1.119	7.275
Original Input $\hat{x}_0$				
Other Condition $C$	None	No state cycle	None	None
State Transition $T$	History features shift by one value			None
Post-condition $Q$	Forall $N(x_i) < 0$	Exist $N(x_i) \approx 0$	Exist $N(x_0) > 0$	Exist $N(x_0) < 0$
$\langle a, b, c \rangle$	$\langle 0.60, 0.40, 0.87 \rangle$	$\langle 0.00, 0.10, 0.17 \rangle$	$\langle 2.20, 1.20, 0.16 \rangle$	$\langle 0.40, 0.90, 0.92 \rangle$
Distance(Euclidean)	1.130	0.199	2.511	1.348
Reinifier Result				
$\langle a, b, c \rangle$	Not applicable	Not applicable	$\langle 2.20, 1.20, 0.16 \rangle$	$\langle 0.40, 0.90, 0.9 \rangle$
UINT Result				

Table 8: Aurora counterfactual explanation questions and comparison of their results by Reinifier and UINT.

	Input 1	Input 2	Input 3	Input 4
$\langle i, l, r \rangle$	$\langle 0.00, 1.00, 1.00 \rangle$	$\langle 0.00, 1.00, 2.00 \rangle$	$\langle 0.00, 2.00, 1.00 \rangle$	$\langle 0.00, 2.00, 2.00 \rangle$
Original Input $\hat{x}_0$				
$N(x_0) \not\approx N(\hat{x}_0)$ Level 1	$\epsilon = 1 \times 10^{-0}$	$\epsilon = 1 \times 10^{-0}$	$\epsilon = 1 \times 10^{-0}$	$\epsilon = 1 \times 10^{-0}$
$N(x_0) \not\approx N(\hat{x}_0)$ Level 2	$\epsilon = 1 \times 10^{-1}$	$\epsilon = 1 \times 10^{-1}$	$\epsilon = 1 \times 10^{-1}$	$\epsilon = 1 \times 10^{-1}$
$N(x_0) \not\approx N(\hat{x}_0)$ Level 3	$\epsilon = 1 \times 10^{-2}$	$\epsilon = 1 \times 10^{-2}$	$\epsilon = 1 \times 10^{-2}$	$\epsilon = 1 \times 10^{-2}$
$N(x_0) \not\approx N(\hat{x}_0)$ Level 4	$\epsilon = 1 \times 10^{-3}$	$\epsilon = 1 \times 10^{-3}$	$\epsilon = 1 \times 10^{-3}$	$\epsilon = 1 \times 10^{-3}$

Table 9: Aurora importance analysis questions.

this property indeed only has one breakpoint for  $var \in [1, 100]$  after linear search. Consequently, the model also passes the intuitiveness examination on this qualitative property. Notably, this result indicates the upper bound of the output constrained by the given input.

$\phi_{9.c}$ : This property is derived from  $\phi_9$ . **Qualitative property:** A higher latency ratio, which implies higher latency, is associated with a greater likelihood of the sending rate immediately decreasing. The result shows that this property only has one breakpoint for  $var \in [1, 100]$  following linear stepping. Consequently, the model also passes the intuitiveness examination on this qualitative property. Besides, the result indicates that the send rate decreases only when the latency ratio is significantly high.

**Counterfactual explanation.** Based on the previous properties of Aurora, we conduct the searches for the closest counterexamples that lead to altered verification results. The questions posed and their results are illustrated in Table 8.

Taking  $\phi_{5.b}$  derived from  $\phi_5$  as an example, the original output is  $-1.119$ ; thus, it proves valuable to seek a counterexample input resulting in an output greater than 0. Remarkably, the result demonstrates that the Euclidean distance to the closest counterexample amounts to 2.511.

Indeed, as outlined in the counterfactual explanation section of the main text, this approach can also be applied to safety and liveness properties. For instance, consider  $\phi_{7.a}$  derived from  $\phi_7$ , and since  $\phi_7$  is verified to be satisfied, we can proceed to search for its counterexamples. In this case, we are interested in finding inputs where the output is approximately 0, and we can gain insights into the conditions under which the sending rate might remain unchanged.

**Importance analysis.** Indeed, the assessment of feature importance can be influenced by how output changes are defined. In cases where the output is a floating-point number, like in Aurora, defining the extent of change in  $N(x_0)$  compared to  $N(\hat{x}_0)$  becomes crucial. To address this,

	Input 1	Input 2	Input 3	Input 4
$\langle i, l, r \rangle$	$\langle 0.00, 1.00, 1.00 \rangle$	$\langle 0.00, 1.00, 2.00 \rangle$	$\langle 0.00, 2.00, 1.00 \rangle$	$\langle 0.00, 2.00, 2.00 \rangle$
Original Input $\hat{x}_0$				
Perturbation Level 1	$\varepsilon = 1 \times 10^{-0}$	$\varepsilon = 1 \times 10^{-0}$	$\varepsilon = 1 \times 10^{-0}$	$\varepsilon = 1 \times 10^{-0}$
Perturbation Level 2	$\varepsilon = 1 \times 10^{-1}$	$\varepsilon = 1 \times 10^{-1}$	$\varepsilon = 1 \times 10^{-1}$	$\varepsilon = 1 \times 10^{-1}$
Perturbation Level 3	$\varepsilon = 1 \times 10^{-2}$	$\varepsilon = 1 \times 10^{-2}$	$\varepsilon = 1 \times 10^{-2}$	$\varepsilon = 1 \times 10^{-2}$
Perturbation Level 4	$\varepsilon = 1 \times 10^{-3}$	$\varepsilon = 1 \times 10^{-3}$	$\varepsilon = 1 \times 10^{-3}$	$\varepsilon = 1 \times 10^{-3}$

Table 10: Aurora sensitivity analysis questions.

	UINT	Reinfier	Benefit
Property Syntax	SMT formula	Intuitive and concise DRLP syntax	Make it easy for users to read and write
DNN Structure	Linear layer and convolutional layer	Almost all structures	Support more DRL systems and adapt to the rapid development of DNN
Result Guarantee	Results from an SMT solver	Comprehensive results from multiple DNN verifiers	Reduce the risk of wrong answer
Type of Property	Robustness	Safety, Liveness, Robustness	Facilitate comprehensive interpretation
Solution	Completely different solutions for different problems	Unified based on <i>break-points</i>	Accelerate total solution speed and facilitate problem extension

Table 11: Advantages of Reinfier compared to UINT.

four different levels of defining change, i.e.,  $N(x_0) \not\approx N(\hat{x}_0) \equiv (N(x_0) \geq N(\hat{x}_0)) \vee (N(x_0) \leq N(\hat{x}_0))$ , have been adopted. This approach provides a range of criteria for determining change and has been applied to four original inputs  $\hat{x}_0$ , as detailed in Table 9.

The evaluation results are shown in Fig. 5. They illustrate that under the four different original inputs discussed, small perturbations of latency inflation lead to output change, and the required perturbation values are much less than the other two features. The relationship between the importance of the latency ratio and the send ratio varies depending on the original input context. However, in the chosen experimental settings, the diverse definitions of  $N(x_0) \not\approx N(\hat{x}_0)$  do not substantially affect the relative importance relationship between the required perturbation values for these three features.

To quantify feature importance, the reciprocal of the perturbation value is employed as the measure of importance. The results illustrate that latency inflation stands out as the most crucial feature in decision-making under these circumstances. This is likely attributed to the fact that the selected original inputs have latency inflation values close to 0, indicating network latency stability. As a result, even a slight perturbation to latency inflation might signify a shift to an unstable network latency condition, prompting the agent to significantly adjust its sending rate.

**Sensitivity analysis.** The sensitivity of features, as measured by the deviation of the output from its original value, varies based on the chosen perturbation levels for the features. To comprehensively analyze this, we employ four dif-

ferent perturbation levels denoted by  $\varepsilon$  and utilize the same set of four original inputs  $\hat{x}_0$  that were used in the Importance Analysis. The perturbation levels, as well as the corresponding original inputs, are listed in Table 10. This approach helps us to explore how different perturbation levels influence the sensitivity of the features under evaluation.

The evaluation results are shown in Fig. 6. They reaffirm the finding that perturbing latency inflation has the most substantial impact on the output, consistent with the observations from the Importance Analysis. Therefore, latency inflation remains the most sensitive feature under the given original inputs. This correlation between importance and sensitivity is reasonable, as important features tend to exhibit higher sensitivity due to their significant influence on the output. The high sensitivity of latency inflation suggests that slight variations in network latency can lead to noticeable changes in the agent’s decision-making. This aligns with the notion that changes in latency may indicate shifts in network stability, prompting the agent to adjust its sending rate accordingly.

**Comparison.** When compared to the interpreter UINT, our *Reinfier* possesses several advantages shown in Table 11. Beyond its benefits in terms of user-friendliness and applicability to a wide range of scenarios, a crucial aspect is our conviction that our cohesive solutions based on *break-points* can be rapidly adapted to new interpretability problems instead of formulating distinct solutions for each individual problem. While the process of searching for *break-points* might be time-consuming, once these breakpoints are

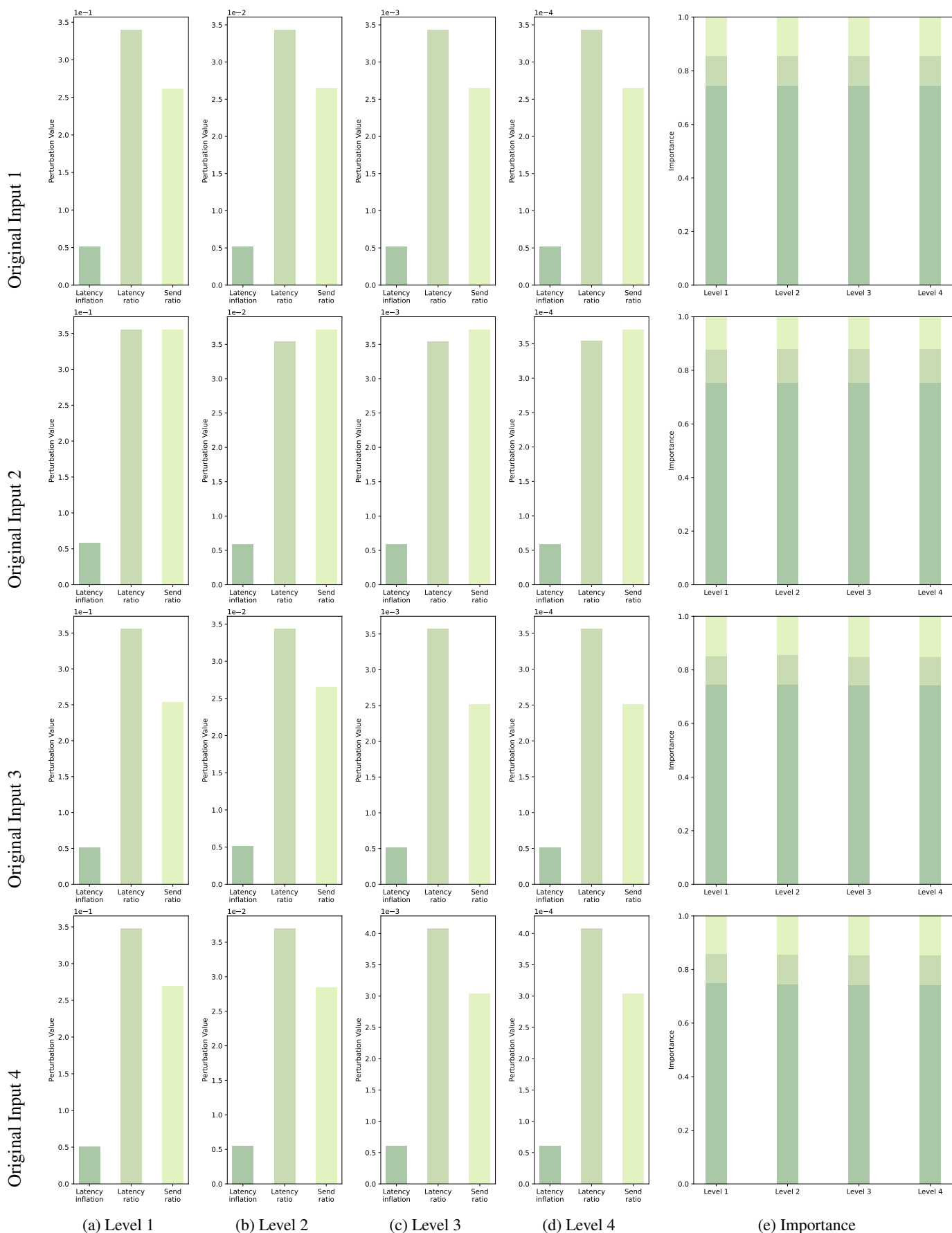


Figure 5: Aurora importance analysis results. Each row indicates different original input  $\hat{x}_0$  as shown in Table 9. The first to fourth columns indicate different  $N(x_0) \not\approx N(\hat{x}_0)$  Levels as shown in Table 9, and the fifth column indicates the proportion of Importance ( $1/\text{Perturbation value}$ ) of each feature under the three features of the input.

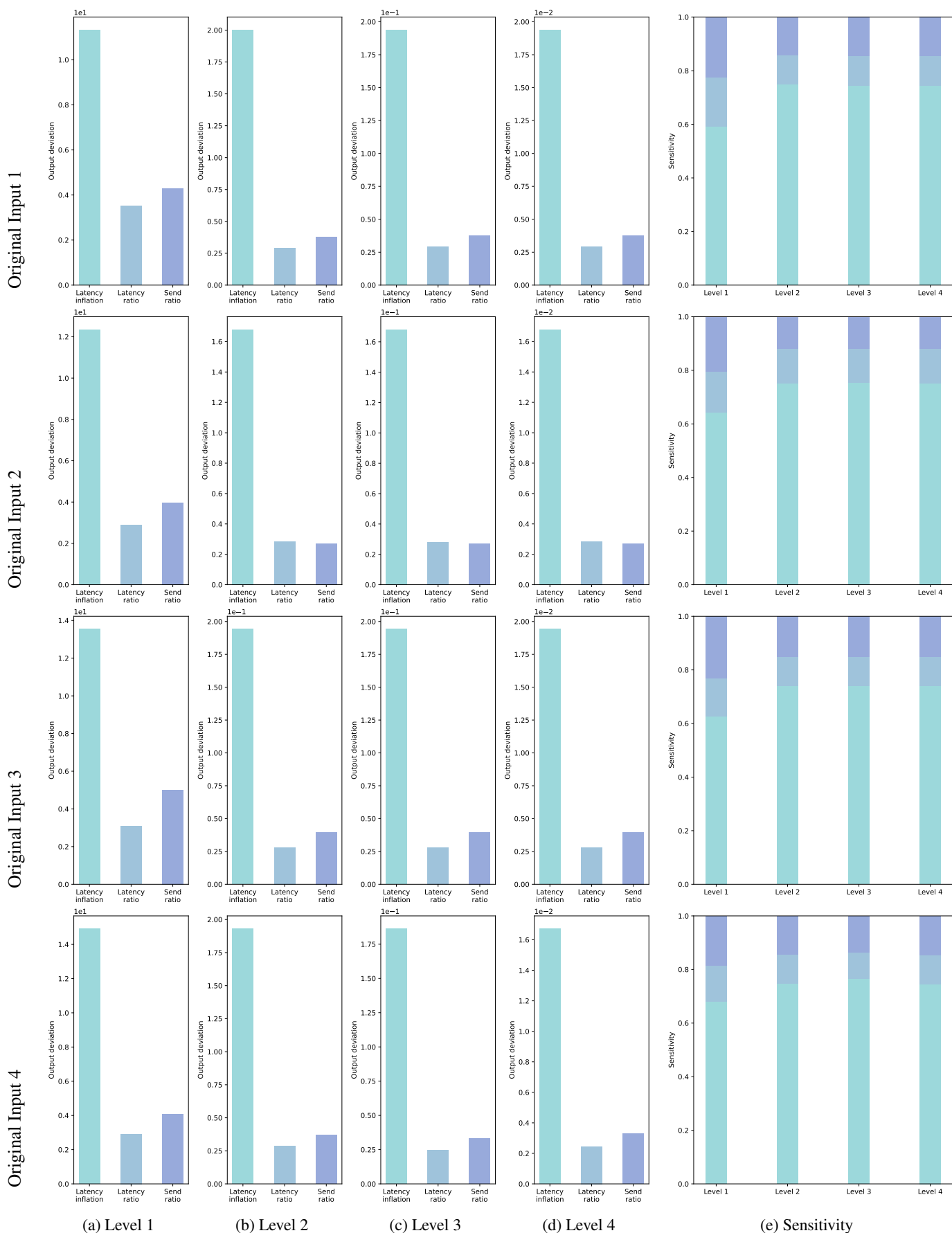


Figure 6: Aurora sensitivity analysis results. Each row indicates different original input  $\hat{x}_0$  as shown in Table 10. The first to fourth columns indicate different Perturbation Levels as shown in Table 10, and the fifth column indicates the proportion of Sensitivity (*Output deviation*) of each feature under the three features of the input.



Task		Mountain Car	Cartpole	Pendulum	
Algorithm		DQN	DQN	DDPG	
ID		$\phi_1$	$\phi_2$	$\phi_3$	
Network	Activation Function	ReLU	ReLU	ReLU	
	Size	$2 \times 256$	$2 \times 256$	300, 400	
Training Time (s)	Reintrainer	878	192	809	
	Trainify#1	443	153	5923	
	Trainify#2	912	144	6209	
	Vanilla	<b>197</b>	<b>60</b>	<b>150</b>	
Timesteps	Reintrainer	$1.0 \times 10^5$	$7.5 \times 10^4$	$1.7 \times 10^4$	
	Trainify#1	$6.3 \times 10^5$	$1.8 \times 10^5$	$8.0 \times 10^5$	
	Trainify#2	$1.3 \times 10^6$	$2.8 \times 10^5$	$8.0 \times 10^5$	
	Vanilla	$1.2 \times 10^5$	<b><math>4.0 \times 10^4</math></b>	<b><math>5.0 \times 10^3</math></b>	
Violations	Reintrainer	<b>96</b>	15	400	
	Trainify#1	668	<b>0</b>	<b>27</b>	
	Trainify#2	1735	<b>0</b>	180	
	Vanilla	117	<b>0</b>	68	

Task		B1	B2	Tora	
Algorithm		DDPG	DDPG	DDPG	
ID		$\phi_4$	$\phi_5$	$\phi_6$	
Network	Activation Function	Tanh	Tanh	Tanh	Tanh
	Size	$2 \times 20$	$2 \times 20$	$3 \times 100$	$3 \times 200$
Training Time (s)	Reintrainer	84	140	491	751
	Trainify#1	304	<b>25</b>	716	797
	Vanilla	<b>80</b>	54	<b>33</b>	<b>48</b>
Timesteps	Reintrainer	<b><math>3.8 \times 10^4</math></b>	$4.8 \times 10^4$	<b><math>9.6 \times 10^3</math></b>	<b><math>9.6 \times 10^3</math></b>
	Trainify#1	$7.7 \times 10^4$	<b><math>1.4 \times 10^4</math></b>	$1.4 \times 10^5$	$1.5 \times 10^5$
	Vanilla	<b><math>3.8 \times 10^4</math></b>	$2.4 \times 10^4$	<b><math>9.6 \times 10^3</math></b>	<b><math>9.6 \times 10^3</math></b>
Violations	Reintrainer	256	128	<b>0</b>	<b>0</b>
	Trainify#1	361	67	<b>0</b>	<b>0</b>
	Vanilla	<b>160</b>	<b>64</b>	<b>0</b>	<b>0</b>

Table 12: Comparison of the training process.

identified, an array of interpretable problems can be answered within seconds. This further underscores the scalability of our solutions.

## E.2 Reintrainer

**E.2.1 Training Process Comparison.** We track the total training time and the numbers of timesteps spent to develop high-performing models as shown in Table 12. The statistics show that the vanilla algorithms have an advantage in total training time, while our approach takes more time due to the inclusion of formal verification and interpretation in training strategy generation. Nonetheless, we strongly believe that this additional time investment is justified, as it substantially increases the reliability of the models. Trainify’s verification method, which treats the DNN as a black box, should have an efficiency edge. However, it is only slightly faster than *Reintrainer* in three benchmarks. Speed improvements of *Reintrainer* can be achieved by parallelizing strategy gen-

eration processes or by reducing their precision.

Nevertheless, our approach holds a significant advantage over Trainify in terms of timesteps in the majority of tasks. This aligns with our approach’s capability to provide precise feedback on reward shaping. It suggests that if the agent runs in an environment with high action costs, our method will still offer advantages in terms of efficiency.

We also track the number of violation occurrences. In conditions where violations occur frequently, such as in  $\phi_1$ , our approach demonstrates advantages in reducing violations. However, when there are few or no violations, such as in  $\phi_2$ , Reintrainer can actively generate a smaller number of counterexamples in the buffer for the agents to learn.  $\phi_3$  is aimed to guide the agent to try to make the pendulum more upright, so more violations occurring during the training process of Reintrainer to promote property satisfaction of the final model are acceptable.

	Vanilla	Const	Raw Dist	Dist	Density	Gap
$\bar{R} \pm \sigma$	-146.53±7.36	-153.65±6.93	-152.88±10.60	-148.61±10.43	-151.94±9.71	-144.79±9.58

Table 13: Ablation experiments of different reward shaping strategies.  $\bar{R} \pm \sigma$  stands for the average episode reward and its standard deviation of the final models’ evaluation results.

Task	Mountain Car	Cartpole	Task	Pendulum	B1, B2	Tora
Algorithm	DQN	DQN	Algorithm	DDPG	DDPG	DDPG
Batch Size	128	64	Buffer Size	200000	10000	10000
Buffer Size	10000	10000	Batch Size	32	32	32
Exploration Final Eps	0.07	0.04	Gamma	0.98	0.99	0.99
Exploration Fraction	0.2	0.16	Tau	0.005	0.02	0.02
Gamma	0.98	0.99	Gradient Steps	200	1	1
Gradient Steps	8	128	Learning Rate	0.001	0.001	0.001
Learning Rate	0.004	0.023	Learning Starts	10000	0	0
Learning Starts	1000	1000	Noise Std	0.1	None	None
Policy	MlpPolicy	MlpPolicy	Noise Type	Normal	None	None
Target Update Interval	600	10	Policy	MlpPolicy	MlpPolicy	MlpPolicy
Train Freq	16 Steps	256 Steps	Train Freq	1 Episode	4 Steps	10 Steps
Normalize	False	False	Normalize	False	False	False

Table 14: Training hyper-parameters of Mountain Car, Cartpole, Pendulum, B1, B2, and Tora.

**E.2.2 Ablation Study** Since there are a significant numerical difference in only the Pendulum task among the six benchmarks, we choose it for the ablation study. We obtain the following reward shaping strategies by selecting whether to enable the metrics in our algorithm.

**Const:** the fixed penalty when the violation is detected; here, we use  $-2$  as the penalty. This strategy can be seen as a purely counterexample-guided training strategy.

**Raw Dist:** the penalty calculated as the sum of distances from the violating state to the property constraint boundary, using Eq.15.

**Dist:** the penalty calculated by using Eq.4 and Eq.5 when a violation is detected, with the density set to 1.

**Density:** the penalty calculated by measuring density using Eq.2 instead of setting it to 1, building on **Dist**.

**Gap:** the penalty calculated by introducing *gap* metric and adjusting the learning rate, building on **Density**; here,  $Lr(gap) = \frac{1}{1+e^{-gap}}$ .

Since  $\phi_3$  is a single-step property, Traceback is not used, and *Gap* represents the complete reward performance of *ReinTrainer* under general conditions.

We independently repeated each penalty condition 20 times and evaluated each with 100 episodes, calculating the mean and variance of the average episode reward over 20 independent repetitions, as shown in Table 13.

Experimental results indicate that our algorithm performs progressively better with more precise metrics and eventually surpasses the fine-tuned vanilla algorithm while ensuring property satisfaction. **Const** is the simplest reward shaping method, using a constant value that makes it difficult for the learning algorithm to estimate the extent of violations,

hence it performs the worst.

**Raw Dist** simply calculates the sum the distances from the violation to the nearest property-constrained, and compared to **Const**, it measures the violation more precisely, thereby showing improved performance.

**Dist** in contrast to **Raw Dist**, calculates the overall distance instead of the sum of distances across individual dimensions and also normalizes the results to prevent issues arising from different dimensional scales, thus making significant advancements to enhance performance.

**Density** introduces density metric, which theoretically should provide more accurate measurements than **Raw Dist**, but the results here show a decline. We analyze that this might be related to the short training cycles of the Pendulum. In this experiment, the `learning starts` parameter is set to 10,000 timesteps, and a good model can be learned by 17,000 timesteps. This means the density calculated before learning starts is meaningless and may interfere with learning. Therefore, when the timesteps from learning start to model convergence are few, the density metric could be disabled.

**Gap** more accurately indicates the progress of property learning, thus reducing the impact of property learning on performance goals when the property learning is close to convergence, i.e., when the *gap* is small. In this experiment, it significantly improved performance even when density performed poorly, highlighting the importance of numerical results from verification for assessing the model’s current state and learning.

**E.2.3 Training Hyper-Parameters** We employ fine-tuned hyper-parameters from Stable Baselines (Raffin et al.

Task	Type	ID	Pre-condition $P$	Post-condition $Q$	Meaning
MC	Safety	$\phi_1$	$p \in [-0.40, -0.60]$ $v \in [0.03, 0.07]$	Forall $Action \neq 0$	When the car is moving at high speed to the right at the bottom of the valley, it should not accelerate to the left.
CP	Safety	$\phi_2$	$p \in [-2.40, -2.00]$ $v \in [0.00, +\infty]$ $\theta \in [0.15, 0.21]$ $\omega \in [1.00, +\infty]$	Forall $Action = 1$	When the car is moving to the right in the left edge area and the pole tilts to the right at a large angle, it should be pushed to the right.
PD	Safety	$\phi_3$	$x \in [0.00, 1.00]$ $y \in [-0.10, 0.10]$ $\omega \in [-0.50, 0.50]$	Forall $Action \in [-1.00, 1.00]$	When the pendulum approaches the upright position of the target, large torque should not be applied.
B1	Liveness	$\phi_4$	$x_0^0 \in [0.80, 0.90]$ $x_0^1 \in [0.50, 0.60]$	Exist $x^0 \in [0.00, 0.20]$ $x^1 \in [0.05, 0.30]$	The agent always reaches the target eventually.
B2	Liveness	$\phi_5$	$x_0^0 \in [0.70, 0.90]$ $x_0^1 \in [0.70, 0.90]$	Exist $x^0 \in [-0.30, 0.10]$ $x^1 \in [-0.35, 0.50]$	The agent always reaches the target eventually.
Tora	Safety	$\phi_6$	$x_0^0 \in [-0.77, -0.75]$ $x_0^1 \in [-0.45, -0.43]$ $x_0^2 \in [0.51, 0.54]$ $x_0^3 \in [-0.30, -0.28]$	Forall $x^0 \in [1.50, 1.50]$ $x^2 \in [1.50, 1.50]$	The agent always stays in the safe region.

Table 15: Predefined properties of benchmarks.

2021) to train models as baselines of vanilla algorithms for tasks Mountain Car, Cartpole, and Pendulum. And we employ the same hyper-parameters from Trainify (Jin et al. 2022) to train models of both vanilla algorithms and Reintrainer for task B1, B2 and Tora. All hyperparameters are shown in Table 14.

**E.2.4 Predefined Properties of Benchmarks.** The detailed definitions of properties in the benchmarks used in the main text are shown in Table 15.

**E.2.5 Transition Dynamics of Benchmarks.** The following benchmarks are not built-in Gym(Brockman et al. 2016) environments. Here are their transition dynamics.

**B1.**  $s_{t+1}^0 = s_t^1, s_{t+1}^1 = a(s_t^1)^2 - s_t^0$

**B2.**  $s_{t+1}^0 = s_t^1 - (s_t^0)^3, s_{t+1}^1 = a$

**Tora.**  $s_{t+1}^0 = s_t^1, s_{t+1}^1 = -s_t^0 + 0.1 \sin s_t^2, s_{t+1}^2 = s_t^3, s_{t+1}^3 = a$

## F Usage

A DRLP object storing a property in DRLP format and an NN object storing an ONNX DNN are required for a DRL verification query in *Reintrainer*. *Reintrainer* can be accessed at <https://github.com/Kurayuri/Reinfier>.

```

1 import reintrainer as rf
2
3 network = rf.NN("/path/to/ONNX/file")
4 # or
5 network = rf.NN(ONNX_object)
6
7 property = rf.DRLP("/path/to/DRLP/file")

```

```

8 # or
9 property = rf.DRLP(DRLP_str)
10
11 # Verify API (default k-induction
12   algorithm, Recommended)
13 result = rf.verify(network, property)
14 # or
15 # k-induction algorithm
16 result = rf.k_induction(network,
17   property)
18 # or
19 # bounded model checking algorithm
20 result = rf.bmc(network, property)
21 # or
22 # reachability analysis
23 algorithm
24 result = rf.reachability(network,
25   property)

```

And the result should be like:

```

1 ( Falsified/Proven/None,
2   an int of verification depth,
3   an violation instance of <numpy.
4   ndarray>)

```

If you want to execute *batch verification*, just run:

```

1 result = rf.verify_linear(network,
2   property)
3 # or
4 result = rf.verify_hypercubic(network,
5   property)

```

If you want to *search breakpoints* and ask interpretability

problems, just run:

```
1 # set search keyword arguments
2 kwargs = {
3     "a": {"lower_bound": -0.7,
4          "upper_bound": -0.3,
5          "precise": 0.02,
6          "method": "linear", },
7     "b": {"lower_bound": 1,
8          "upper_bound": 20,
9          "precise": 0.1,
10         "method": "binary", },
11 }
12 # search breakpoints
13 breakpoints = rf.search_breakpoints(
14     network,property,kwargs)
15
16 # analyze breakpoints
17 inline_breakpoints, inline_breaklines=
18     analyze_breakpoints(breakpoints)
19
20 # answer interpretability problems
21 result = rf.interpreter.
22     answer_importance_analysis(
23         inline_breakpoints)
24 # or sensitivity_analysis
25 result = rf.interpreter.
26     answer_sensitivity_analysis(
27         inline_breakpoints)
28 # or
29 result = rf.interpreter.
30     answer_intuitiveness_examination(
31         inline_breakpoints)
32 #or
33 result = rf.interpreter.
34     answer_counterfactual_explanation(
35         inline_breakpoints)
36 #or
37 result = rf.interpreter.
38     draw_decision_boundary(
39         inline_breakpoints)
```

If you want to use Reintrainer to train a DRL model to satisfy desired DRLP properties, just run:

```
1 reintrainer = rf.Reintrainer(
2     [list of desired DRLP properties],
3     train_api)
4
5 reintrainer.train(max iterations)
```